A Cryosurgical Approach to Lung Cancer

Edgar Allen Cabrera, Kerry Mullaney, Marina Ramirez
BEE 453: Computer-Aided Engineering:
Applications to Biomedical Processes
7 May 2004

I. Executive Summary

Lung cancer is the second leading cause of death in the United States[i], presenting the need for more refined treatment options than traditional invasive surgery and chemo- and radiation therapy. This study investigates the use of less-invasive cryosurgery to effectively freeze and kill a cancerous lung tumor, 3mm in diameter, while minimizing peripheral tissue damage. A single, liquid-nitrogen filled probe is inserted into a lung tumor and maintained at a constant temperature of -190°C. The freezing front is monitored to ensure cancerous cell death and prevent excessive damage to the surrounding healthy tissue. Based on data obtained by analyzing probe temperature, contact time and model sensitivity to variations in biomaterial properties, recommendations are made for surgical implementation: an initial contact time of 6 minutes followed by successively shorter application times. Additionally, further study designs are discussed to improve the quality of this treatment method and to ensure target outcomes with respect to tumor cell death and protection of healthy lung tissue.

II. Introduction and Design Objectives

Background Information

Cancer is the second leading cause of death in America, with lung cancer having the greatest occurrence. This year there will be 175,000 more cases diagnosed in the United States alone[i], further expressing the need for more effective methods of treatment. While previous removal procedures include Chemical and Radiation Therapy, and Traditional and Laser Surgery, perhaps a cryosurgical approach would be most successful.

Since its original application in 1961, advancements in cryosurgery have presented a relatively noninvasive alternative to traditional surgery for treating both malignant and benign tumors in the lungs. By inserting one or more liquid nitrogen-filled cryoprobes into an affected area, surgeons can achieve localized freezing of unhealthy tissue, while causing minimal damage to the surrounding areas. Target freezing temperatures for such procedures range from approximately 233K[ii] to 248K[iii].

Design Objectives

In this study, the optimal cryoprobe application time to effectively freeze a cylindrical cancerous mass in the lung, while minimizing damage to the surrounding healthy tissue was determined. Additionally, the effects of input value modifications with respect to tissue properties and analysis parameters on probe contact time were investigated. Simulations were conducted used the computer programs Gambit and FIDAP.

Problem Schematic

The region of interest was modeled as a cylindrical probe within a cancerous cylindrical mass having, with the exception of specific heat, uniform properties. The tumor was assumed to be completely encompassed by a continuous cylinder of healthy tissue having its own properties. Analysis was further simplified by modeling the systems as 2-dimensional quarter circle (Figure 15.).

III. Results and Discussion

Assumptions

In the process of modeling cryosurgery in this case a few simplifying assumptions were made. These include:

- An approximation that the apparent specific heat of lung tissue was equivalent to that of beef.
- The densities of the tumor and healthy tissues were assumed to stay constant throughout the process.
- The thermal conductivities of the tumor and healthy tissues were assumed to stay constant throughout the process.
- Both the constant thermal conductivity and density properties were approximated by average known values of frozen and unfrozen properties.
- All input properties were homogeneous throughout their respective tissues.
- Blood flow does not affect heat transfer at these temperatures.
- The tumor was perfectly circular.

- The temperature of the tissue and tumor were initially the same, 37°C.
- The maximum temperature to effectively kill the tumor cells is -25 °C[iii].
- Bioheat generation contributions were negligible at such depressed temperatures[ivv].
- There is a clear distinction between a tumor and its surrounding healthy tissue.
- Formation of an ice ball around the probe during the freezing process required variations in apparent specific heat during the phase change process to be accounted for[vi].

Mesh

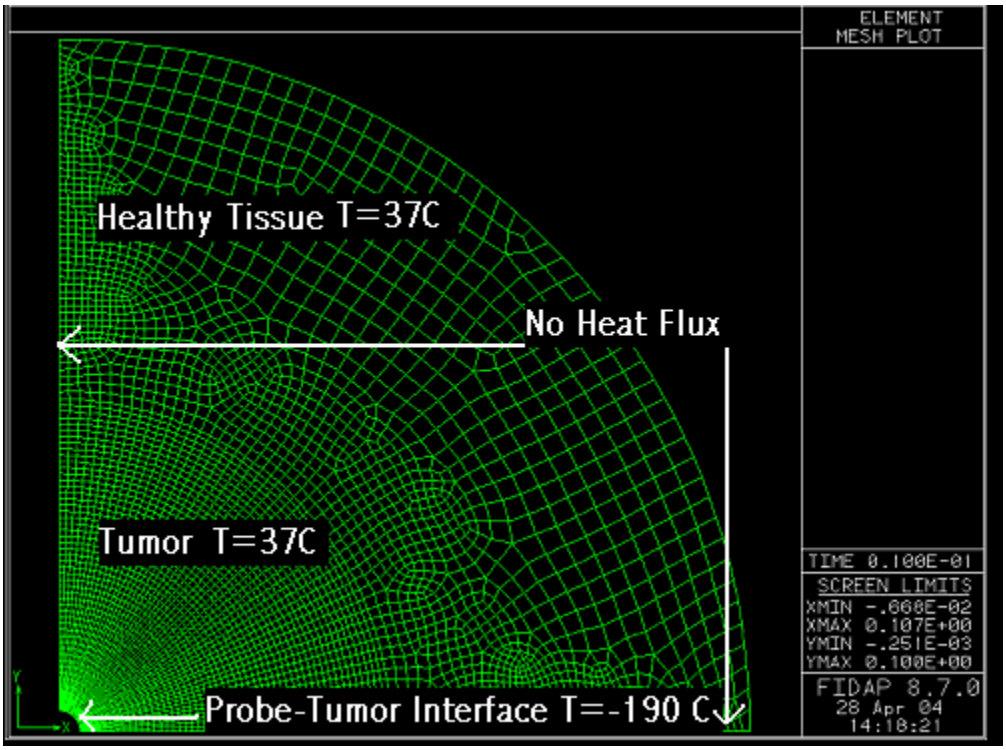

Figure 1. Mesh used for FIDAP simulations; generated in Gambit.

When applying the probe to the tumor tissue, you want to optimize tumor cell death and minimize the damage to the healthy tissue. For this reason an optimal time occurs at which the most damage occurs to the tumor with the least damage to the healthy tissue. In this analysis, data was obtained for a constant application of a cryosurgery probe over an extended period of time. As seen in Figures 2 through 4 below, the progression of the freezing front occurs over a period of time. Figures 27 and 28 in Appendix C display temperature contours at progressively later times.

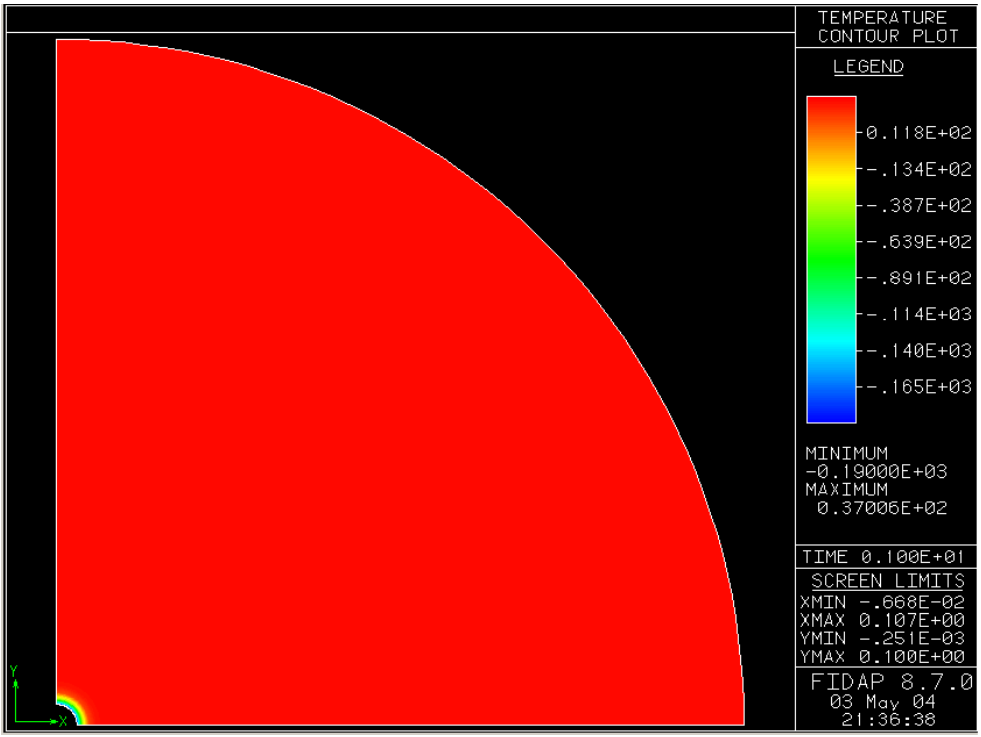

Figure 2. Temperature contour after the application of the probe for one second.

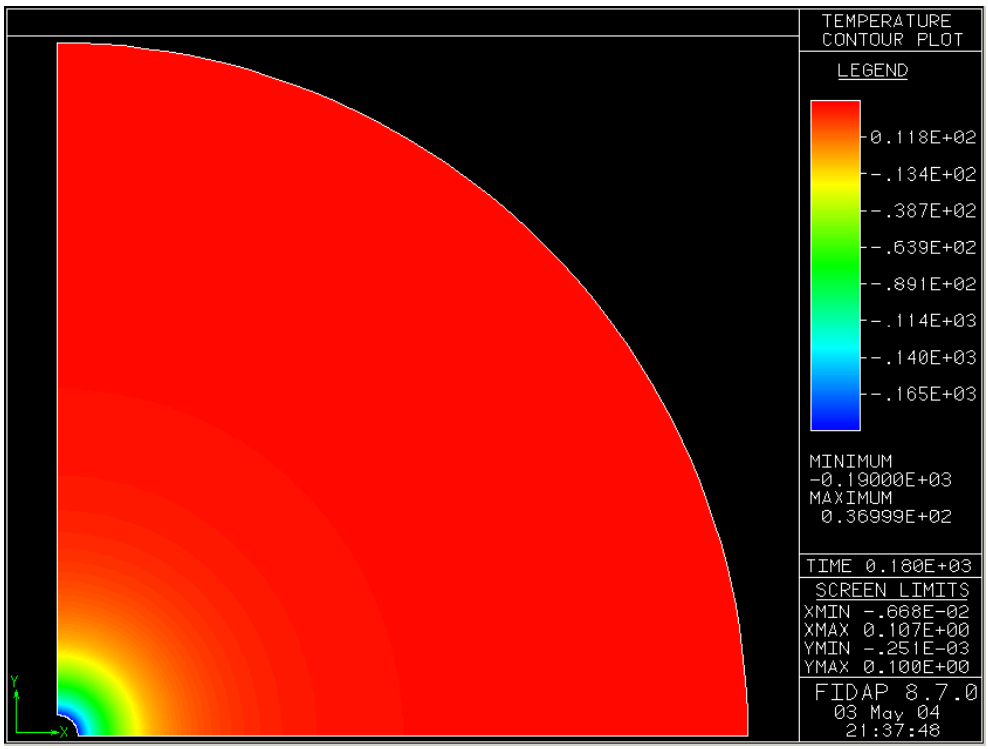

Figure 3. Temperature contour after application of the probe for three minutes.

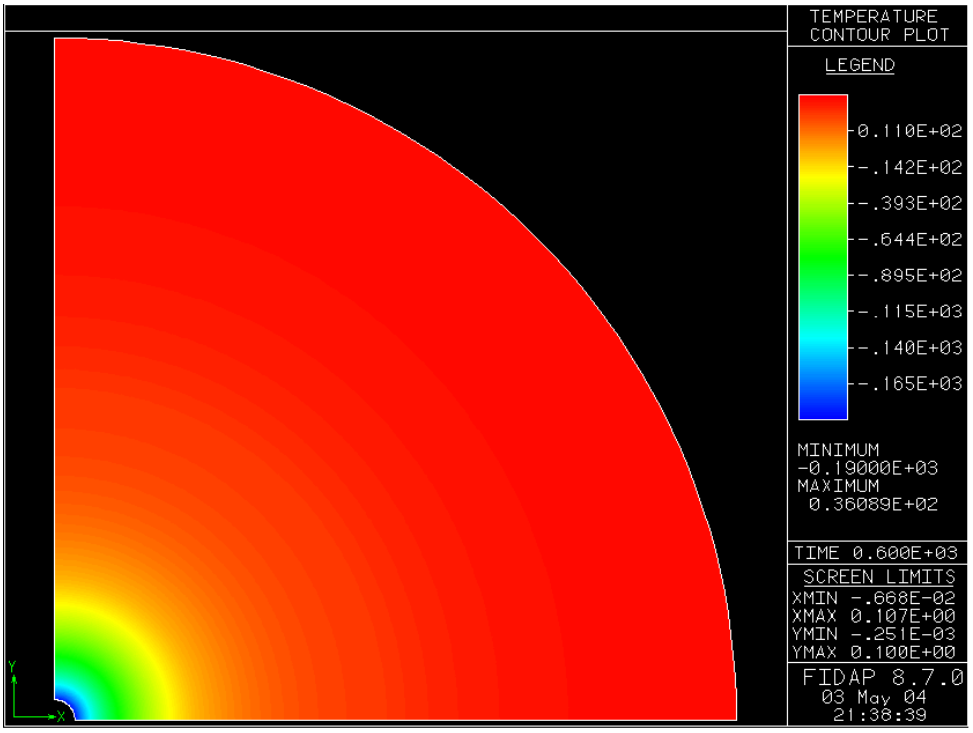

Figure 4. Temperature contour after application of the probe for ten minutes.

These results point to the conclusion that one application of the probe causes extended damage to the surrounding tissues. We reasoned from the obtained data that the best method would be to apply the probe for an optimal time to cause the most damage to the tumor but the least damage to the tissue, then remove the probe and successively reapply it for decreasing amounts of time. The reasoning behind the lag time between applications, is to allow for dissipation of heat within the tissue farthest away from the application point. In this approach, applying the probe for less and less time would account for the change in amount of living tumor tissue. As the amount of unfrozen tumor tissue decreases application must also decrease otherwise damage will occur in the healthy tissue as the freezing front propagates through the tissues. To determine an optimal application time, we compared the history plots of nodes 1247, 275 & 2688 within the mesh. These nodes occur near the edge of the tumor, the beginning of the healthy tissue, and the end of the tumor, respectively. For the specific location refer to Figure 26 in Appendix C. From these graphs a qualitative analysis of tissue temperature to tumor damage has an optimal probe application of six minutes, for a tumor of this diameter; this is a safe estimate. Application could last as long as 10 minutes without significant damage to the lung tissue. If the tumor radius were smaller, this time would decrease.

Sensitivity Analysis

A sensitivity analysis was performed to estimate how dependent the results of this model were on the material properties. This analysis allowed us to estimate how accurate our results are. The sensitivity analysis included altering the density of the tissue surrounding the tumor, the temperature of the probe applied to the tumor, and the apparent specific heat values. The first step was to first refine our mesh and confirm convergence. Figures 17-22 display the convergence of our mesh in Appendix B. Modeling the freezing process with this mesh cause no appreciable change in the data collected.

The first step in our analysis was in increase the density of the surrounding healthy tissue. The density of lung tissue is very low due to the function of the tissue it is very porous. We wanted to see the affects of increasing the density on the time it takes to freeze the tumor and consequently the optimal application time. When we increased the density we performed an analysis on both a higher density less than the density of the tumor and a density greater than the density of the tumor. This way we could eliminate any factors due to the density of the tumor being greater than the surrounding tissue. The following figures show the temperature history of a node at the outer edge of the tumor, for all three densities.

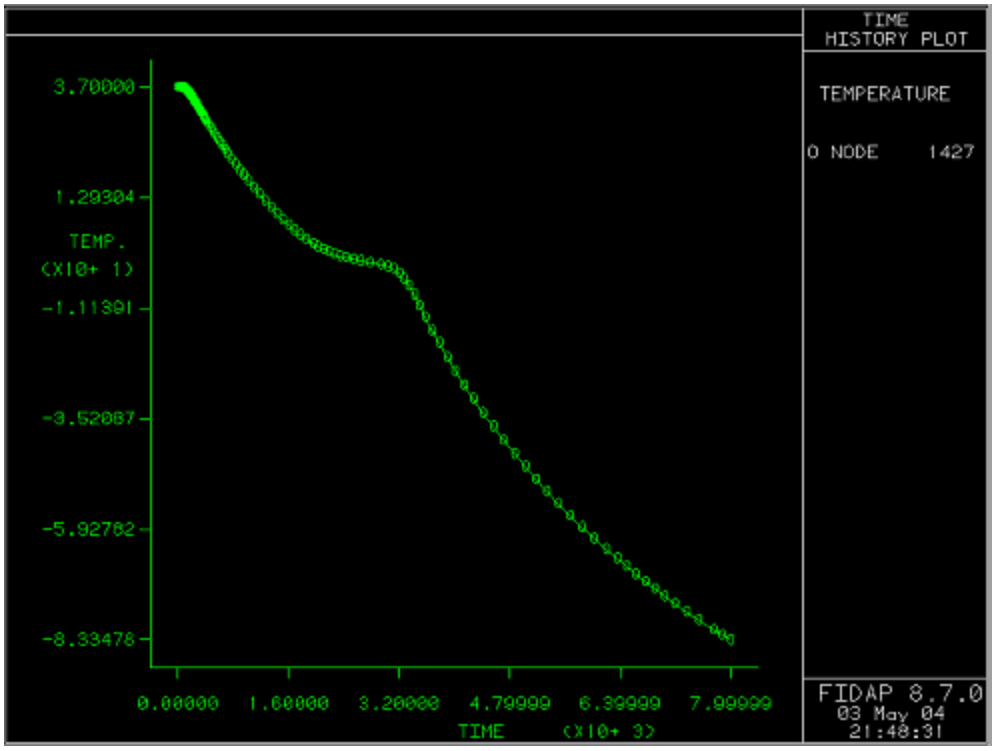

Figure 5. Temperature history of node 1427 on the outer edge of the tumor with surrounding healthy tissue having a density of 200kg/m^3.

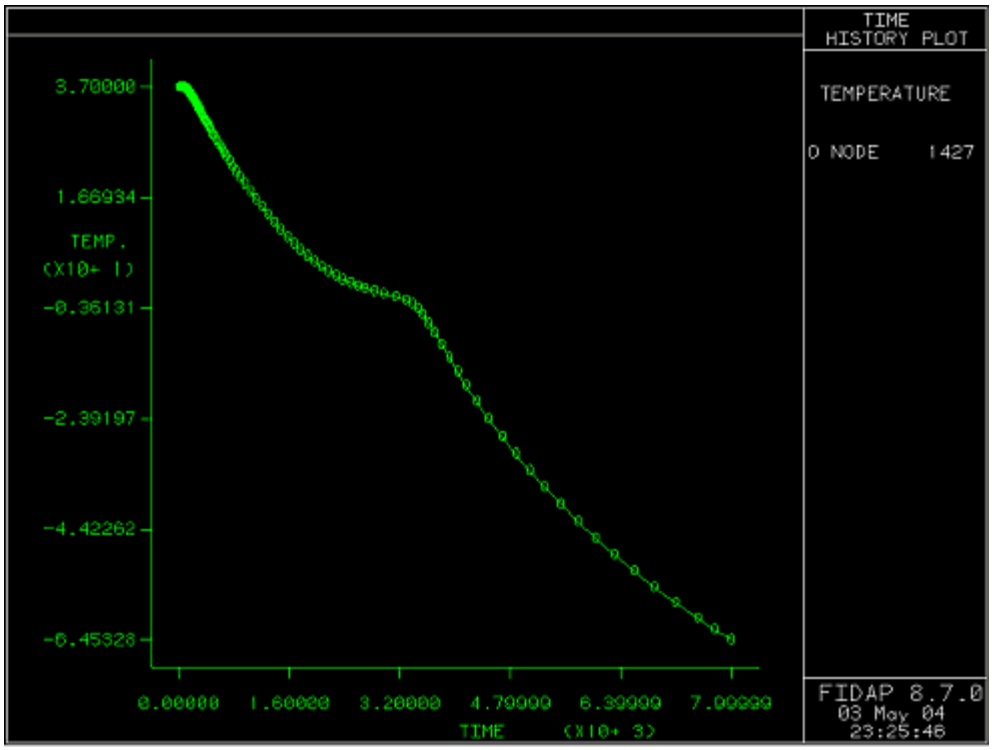

Figure 6. Temperature history of node 1427 at the outer edge of the tumor, with surrounding healthy tissue having a density of 500kg/m^3.

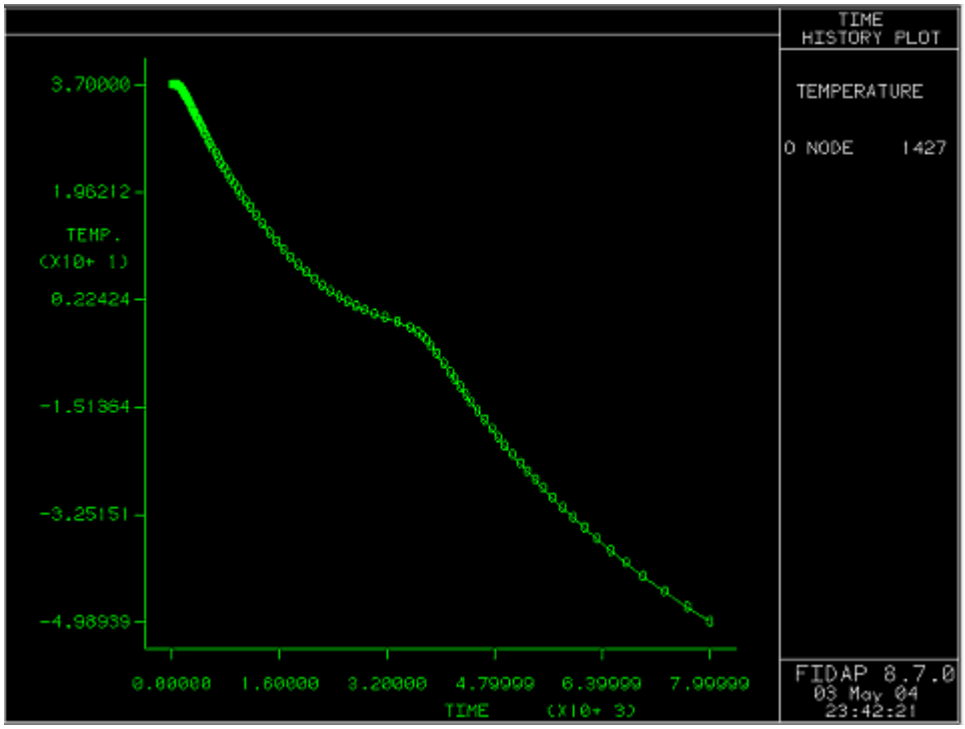

Figure 7. Temperature history at node 1427 on the outer edge of the tumor, with surrounding healthy tissue having a density of 1000kg/m^3.

The shapes of the graphs are extremely similar and freezing occurs at about the same time for each. However, more than doubling then tripling the density of the surrounding healthy tissue produces a minimal effect on the freezing temperature. Although, there is a difference in the temperature of after 8000 seconds; it is warmer at the outer edge of the tumor as the surrounding density increases. However, this change in temperature is on the same order of magnitude. Further analysis of the temperature history at a node just on the inside of the healthy tissue and at the outer edge of the tumor tissue reveal that this trend not only continues but is amplified as you move further into the healthy tissue. Refer to Figures 37-39 in Appendix C. It can be concluded from this data that the density of the surrounding tissue will not affect the time necessary to freeze the tumor nor the temperature of the tissue after freezing. There were large changes in density but the temperature was on the same order of magnitude that is expected. So the model is insensitive to changes in the density of the healthy tissue directly. Rather, the denser the surrounding healthy tissue, the more the tissue will be able to insulate itself against the change in temperature. The damage occurred to the healthy tissue is much less in denser tissue. This in turns means that the application time of the probe can increase and not result in a significant change in the damage that occurs to the healthy tissue. Our model's application time is then only indirectly sensitive to the density of the surrounding tissue.

The results of the density sensitivity analysis was both expected and unexpected. We believe that a change in the density of the surrounding healthy tissue would have an appreciable affect on the freezing time of the tumor. The logic was that the surrounding tissue would act as an insulator to keep the tumor at 37 °C. This was not the case though. The results, although not what was expected, do make sense. Close to the probe the tumor tissue can be modeled as infinitely far from the healthy tissue and so it would not have an affecting on freezing at this point. The majority of the tumor freezes in this manner and results in little sensitivity of the freezing time to healthy tissue density. With respect to the temperature of the healthy tissue, the results were as expected. As this tissue becomes denser it will act like an insulator and be more difficult to cool down.

Next we performed an analysis on the temperature of the probe. We investigated this to see if changing the probe temperature dramatically changed either the time to freeze or the optimal application time. We increased and decreased the probe temperature to –175 and –240 °C, respectively. The following figures show contour after three minutes of application for the two different temperatures. (Refer back to Figure 3 for a contour for the normal temperature after three minutes)

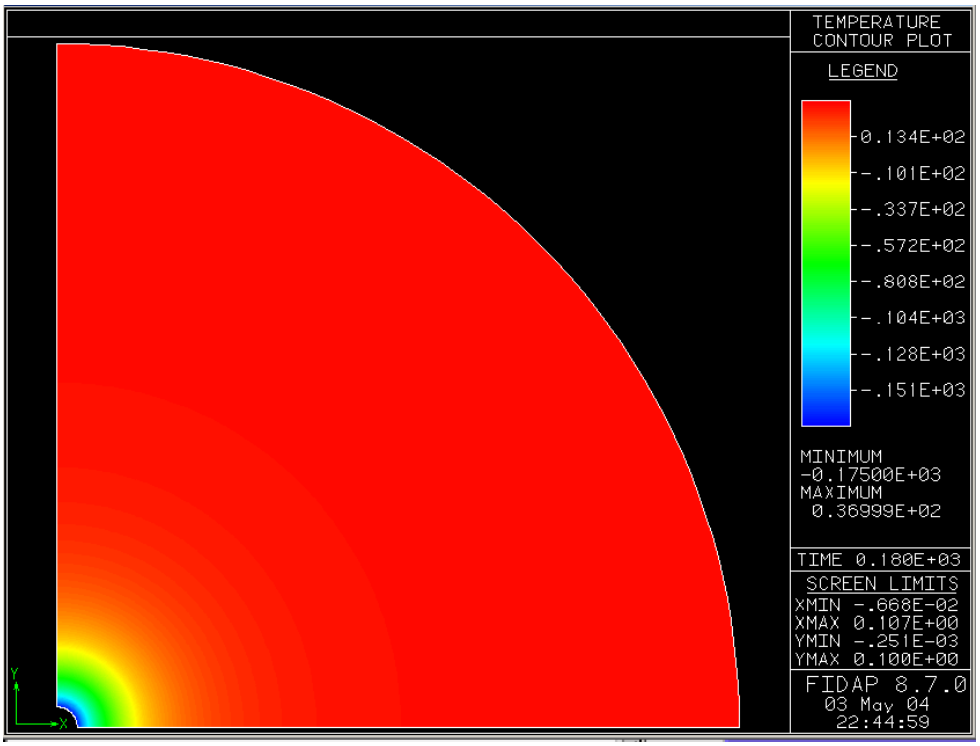

Figure 8. Temperature contour after three minutes of application with a probe temperature of –175 °C.

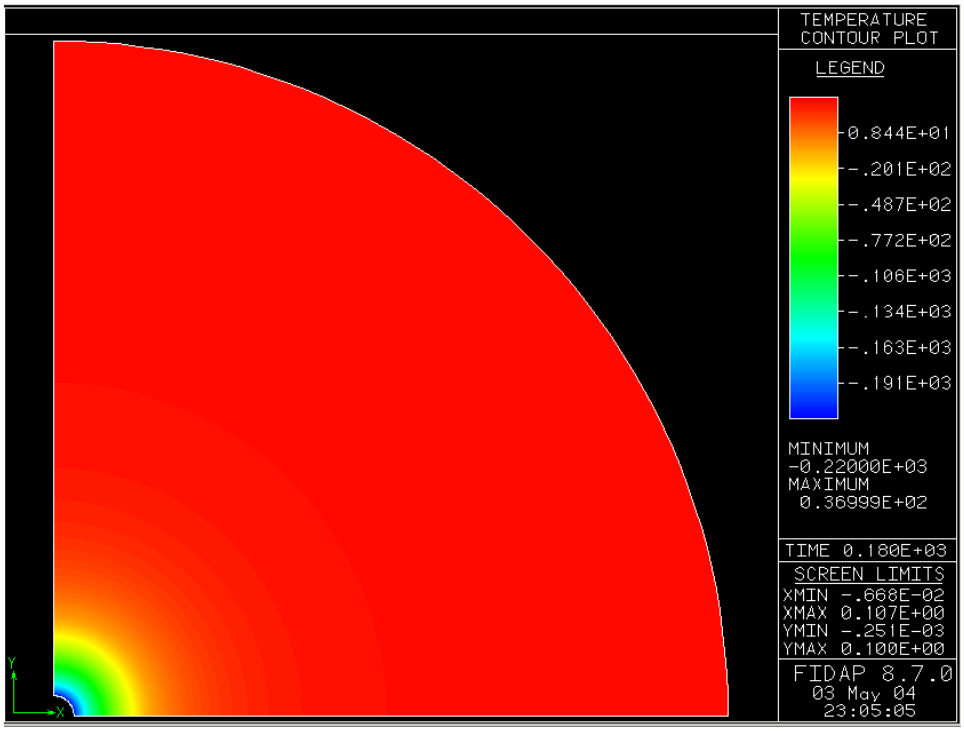

Figure 9. Temperature contour after three minutes of application with a probe with a temperature of –240 °C.

The graphs appear very similar but looking at the legend it becomes clear they are scaled very differently. Other contours at various times and temperature history plots at pivotal points in the mesh were obtained and are located in Appendix C (Figures 31-36). From both the history plots and the contours it can be seen that a change in probe temperature will as expected have a change in the time it takes to freeze the tumor. The change is temperature was about a 10 % increase and a 25 % increase. This resulted in about a 13% increase and 15% decrease in time respectively. For this it can be determined that our model is not sensitive to the temperature of the probe; significant changes in temperature result in only changes in freezing time of about the same significance. We did not expect our model to be extremely sensitive to the temperature of the probe due to the size of the tumor we are modeling.

Finally, we performed a sensitivity analysis on the apparent specific heat values we determined. Originally, we used enthalpy values obtained from a graph for beef temperatures during freezing. We divided the slope of the graph by the change in temperature it occurred over to arrive at apparent specific heat values. From the beginning we knew these were not accurate for out tissue. After further research we discover some specific heat values for lung tissue when both frozen and unfrozen. The beef values had been underestimating in the frozen regime and underestimating in the unfrozen regime. The following graph compares the data used originally and in the sensitivity analysis.

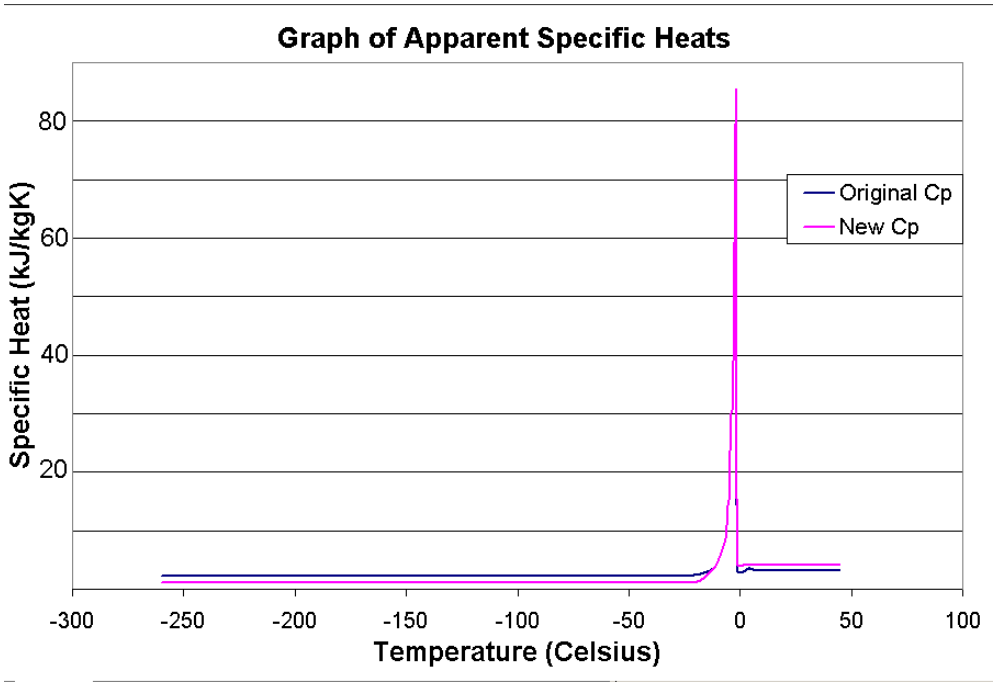

Figure 10. Comparison of original apparent specific heat values, those of beef muscle, and values used in the sensitivity analysis, those of lung tissue.

This new apparent specific heat curve was implement into FIDAP. The following data was obtained. (Refer to Appendix C Figures 29 and 30 for a comparison with the original data)

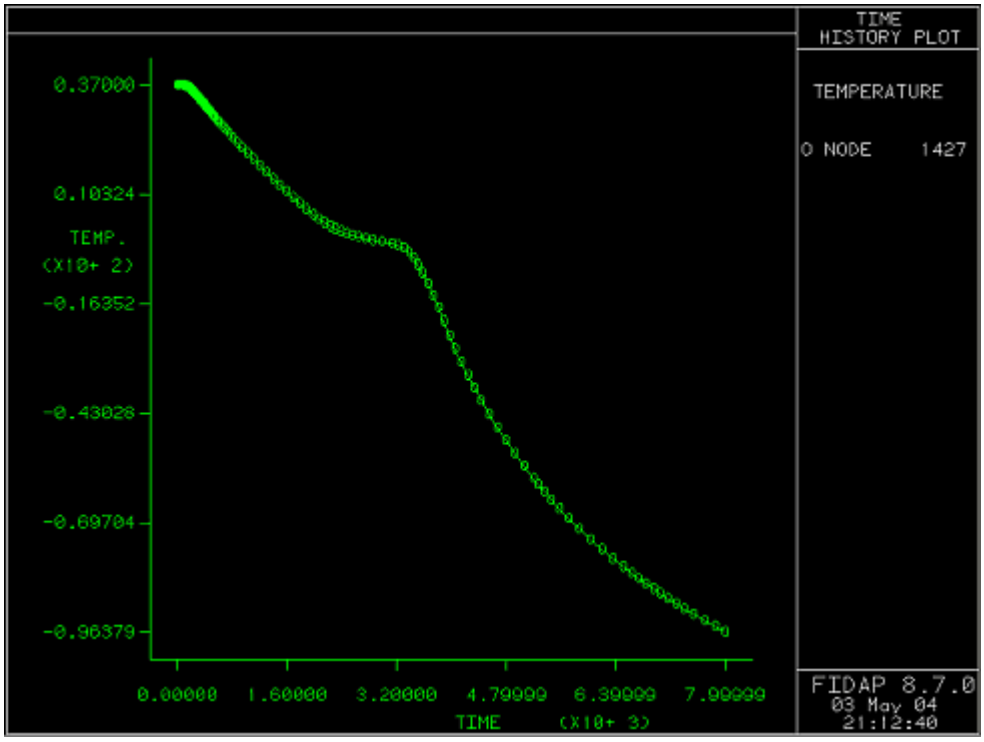

Figure 11. Temperature history curve of node 1427 on the outer edge of the tumor, using the new specific heat curve with values for lung tissue.

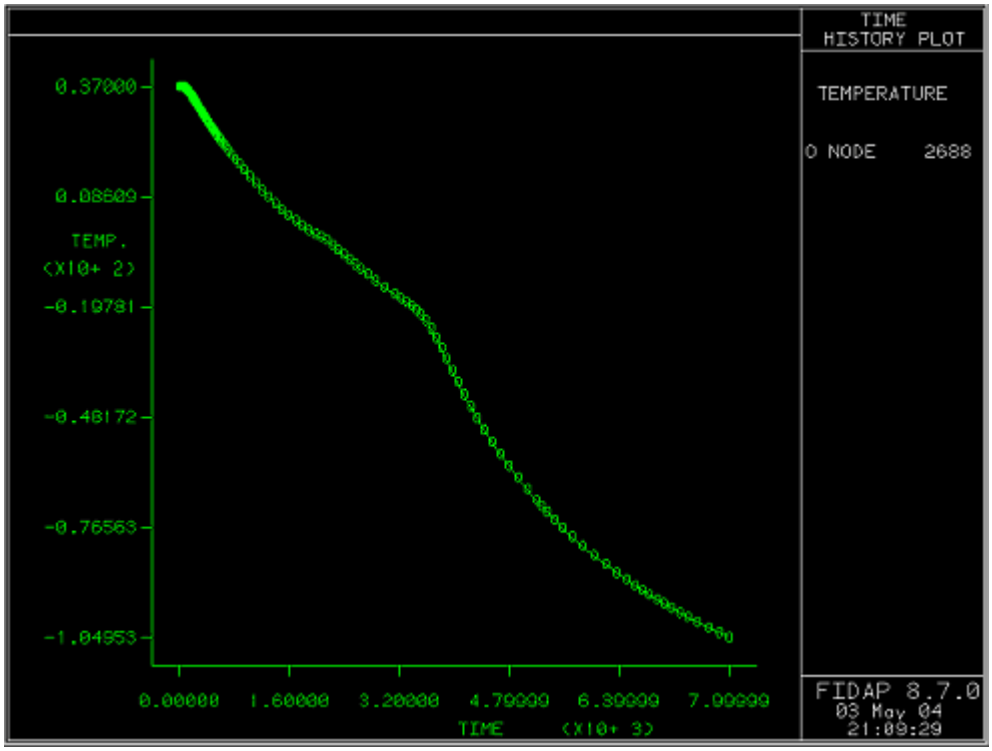

Figure 12. Temperature history profile at node 2688 near the inner edge of the healthy lung tissue, using the new specific heat curve with values for lung tissue..

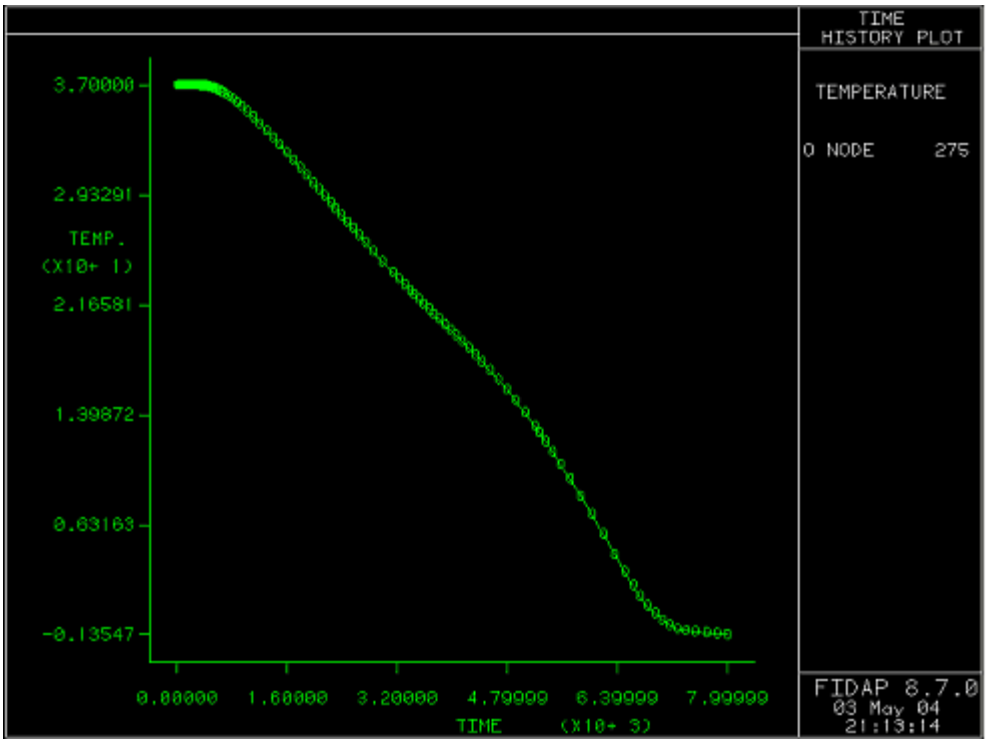

Figure 13. Temperature history profile at node 275 on the outer edge of the healthy tissue, using the new specific heat curve with values for lung tissue.

From the first two graphs a trend is beginning to appear. The bump during freezing is becoming less and less distinct. From a comparison of the original temperature history plots and the plots representing the new specific heat, we determined that the temperature of the healthy tissue in our model is now sensitive to the apparent specific heat. Rather our mode's optimal application time is very sensitive to the apparent specific heat. The optimal application time drops from a safe estimate of 6 minutes with a 10 minute maximum to a maximum application of 6 minutes with a safer standard application time of 3 minuets.

We expected our model to be slightly sensitive to specific heat. We had previously seen the change in time when we originally changed the specific heat from a constant to account for the latent heat. We did not think that our model would be extremely sensitive to this change though since we still accounted for the change of phase in the same manner.

IV. Conclusion and Design Recommendations

It was determined that a safe application time of the cryoprobe to our tumor model is 6 minutes, with a maximum allowable contact time of 10 minutes. Following these guidelines results in a large percentage of tumor cell death, while minimizing damage to the surrounding healthy lung tissue. However, further design recommendations include using multiple probes simultaneously to both decrease application time and increase effective tumor cell death while preserving peripheral tissue. A mesh of this design is illustrated in Figure 14. Additionally, tumors of various shapes and sizes should be modeled and considerations as to the needs for probes of differing geometries should be assessed.

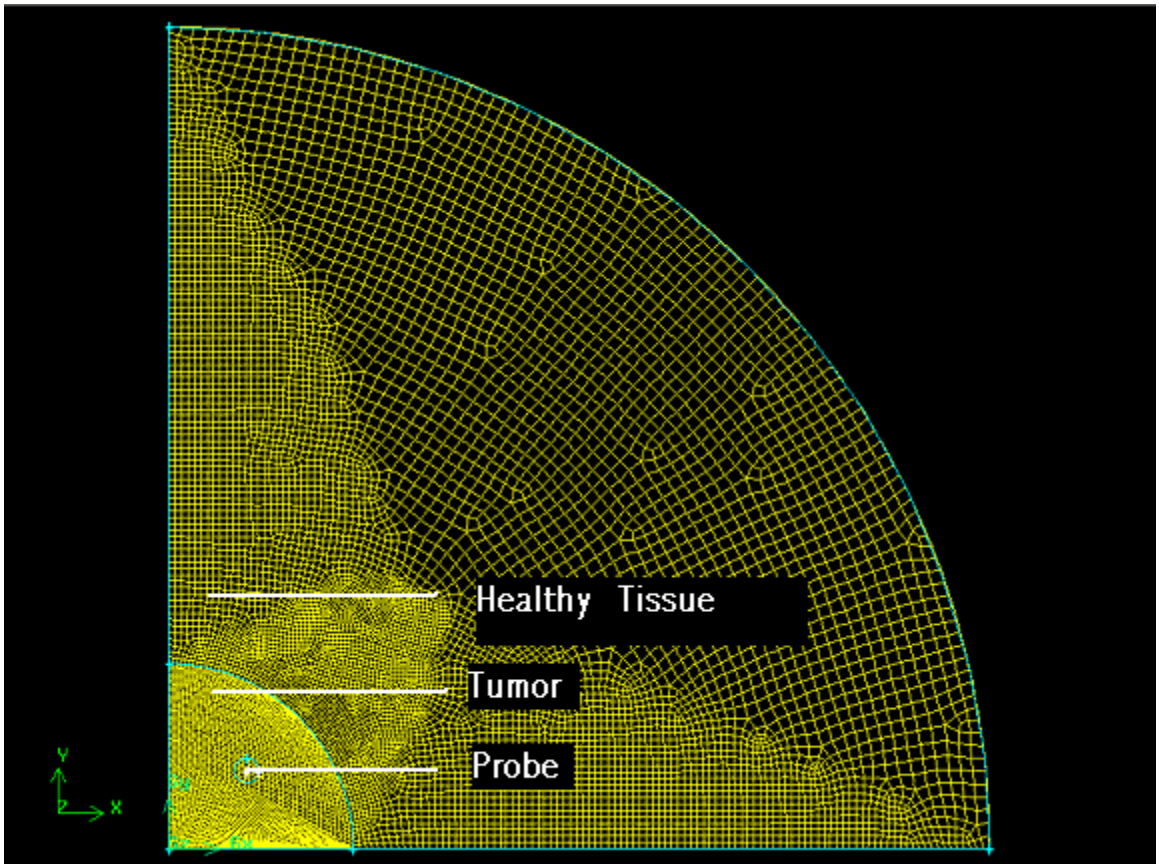

Figure 14. Mesh for the proposed simultaneous usage of four cryoprobes to effectively freeze the lung tumor.

Cost considerations and realistic constraints concerning manufacturability and health and safety were also taken into account. Since most cryosurgical procedures are performed at an in-patient hospital, as opposed to an outpatient center, having multiple probes available should not be difficult. The equipment itself is relatively inexpensive[vii][viii] and with the continued growth in cryosurgery, most medical facilities would have no problem providing sufficient technical support. Since our proposed surgical approach relies on equipment that is already widely used, there will not be any manufacturing problems. Finally, as outlined throughout the study, the patient's health and safety has always been the top priority: the purpose of this study was to kill lung tumor cells while preserving the healthy lung tissue. Doing so results in rapid recovery for the patient with minimal side effects and an overall increase in quality of life.

V. Appendices

Appendix A

Geometry

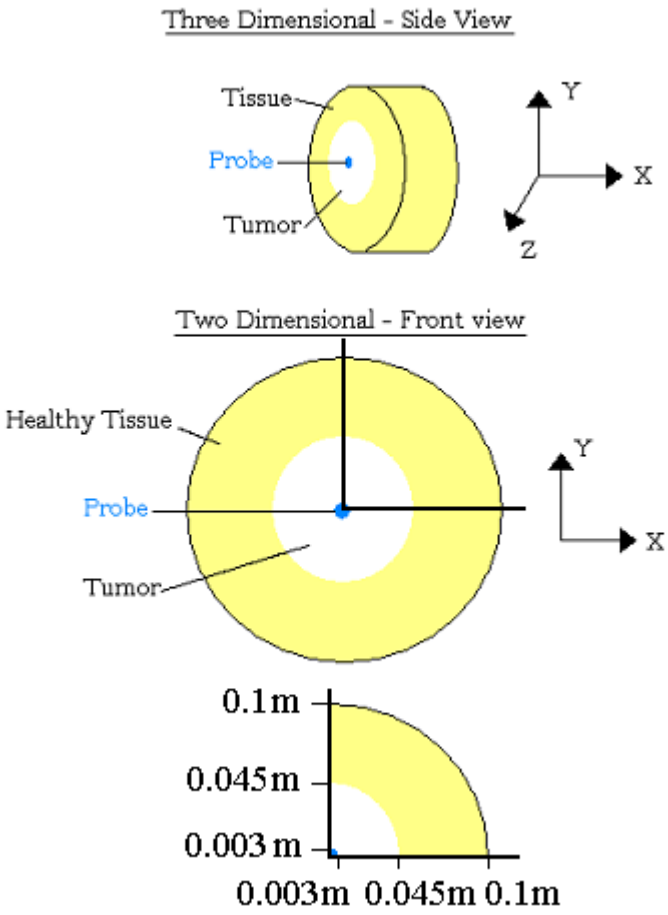

Figure 15. a) 3-Dimensional side view of the model. A cylindrical probe is inserted into a cylindrical tumor that is completely surrounded by healthy lung tissue; the control volume is taken to be a cylinder. b) The simplified 2-dimensional cross section of the model. The probe, tumor, and healthy tissue are concentric circles. c) Quadrant I of the 2-Dimensional frontal view of the model, with element measurements.

Governing Equations

The Energy Equation was used to model tissue temperature as a function of both position and time throughout the tumor and healthy lung tissue

$$\rho c_{p\ apparent} \left(\frac{\partial T}{\partial t} \right) = k \left(\frac{\partial^2 T}{\partial x^2} + \frac{\partial^2 T}{\partial y^2} \right)$$

ρ: density (kg/m^3)
c_{pa}: apparent specific heat (kJ/kgK)
k: thermal conductivity (W/mK)
T: temperature (K)
t: time (s)

Equation for the apparent latent specific heat:

$$dH = \underbrace{[\underbrace{(1-w)c_{p_s}}_{SolidMatrix} + \underbrace{w((1-f)c_{p_w}}_{Water} + f * \underbrace{c_{p_i}}_{Ice})]dT}_{SpecificHeat} - \cancel{\underbrace{\lambda df w}_{LatentHeat}}$$

H: Enthalpy per unit mass (J/kg)
w: Fraction of water
f: Fraction of ice
λ: Latent heat of freezing (J/kg)

This equation reduces to:

$$dH = (c_{Papparent})\, dT$$

Initial and Boundary Conditions

Initial Temperature of both Tumor Tissue and Healthy Tissue = 37 °C.
The heat flux at all the edges was set equal to 0 J/m^2, insulated.

Input Parameters

TissueType	Radius (m)	Thermal Conductivity (W/mK)	Density (kg/m^3)
Tumor	0.045	1.401	200
Healthy	0.200	0.245	960

Temperature (°C)	Specific Heat (J/kg)
-200	2.321
-50	2.321
-28.9	2.321
-23.3	2.321428571
-17.8	2.709090909
-12.2	3.607142857
-9.4	5.321428571
-6.7	8.703703704
-5.6	13.27272727
-4.4	17.58333333
-3.9	29.4
-3.3	32.16666667
-2.8	52.6
-2.2	65.5
-1.7	83.4
-1.1	3
1.7	3
4.4	3.518518519
7.2	3.178571429
10	3.214285714
15.6	3.160714286
37.1	3.16

x

Appendix B

Problem Statement

Geometry Type - 2D
Flow Regime - Incompressible
Simulation Type - Transient
Flow Type - Laminar
Convective Term – Linear
Fluid Type - Newtonian
Momentum Equation – NoMomentum
Temperature Dependence – Energy
Surface Type – Fixed
Structural Solver – NoStructural
Remeshing – NoRemeshing
Number of Phase - Single

Solution Statement

Solution Method – Successive Substitution = 10
Relaxation Factor – ACCF = 0

Time Integration Statement

Time integration - Backward
No. time steps Nsteps = 900
Starting time Tstart = 0
Ending time Tend = 8000
Time increment dt = 0.01
Time stepping algorithm Variable = 0.01
Max Increase Factor Incmax = 1.2

FIINP FILE

```
/
/  INPUT FILE CREATED ON 03 May 04 AT  20:41:36
/
/
/ ***  FICONV Conversion Commands ***
/ ***  Remove / to uncomment as needed
/
/  FICONV(NEUTRAL,NORESULTS,INPUT)
/  INPUT(FILE= "apr28.FDNEUT")
/  END
/  *** of FICONV Conversion Commands
/
TITLE
/
/ ***  FIPREP  Commands ***
/
FIPREP
 PROB (2-D, INCO, TRAN, LAMI, LINE, NEWT, NOMO, ENER, FIXE, NOST,
NORE, SING)
 EXEC (NEWJ)
 SOLU (S.S. = 10, ACCF = 0.000000000000E+00)
 TIME (BACK, NSTE = 900, TSTA = 0.000000000000E+00, TEND = 8000.0,
      DT = 0.100000000000E-01, VARI = 0.100000000000E-01, INCM = 1.2)
 ENTI (NAME = "LUNGFACE", SOLI, MDEN = "tissue", MSPH = 1, MCON =
"Lung")
 ENTI (NAME = "TUMB", PLOT)
 ENTI (NAME = "LUNGB", PLOT)
 ENTI (NAME = "TUML", PLOT)
 ENTI (NAME = "LUNGL", PLOT)
 ENTI (NAME = "PROTUM", PLOT)
 ENTI (NAME = "TUMLUNG", PLOT)
 ENTI (NAME = "LUNGEND", PLOT)
 ENTI (NAME = "TUMORFACE", SOLI, MDEN = "tumor", MSPH = 1, MCON =
"Tumor")
 DENS (SET = "tumor", CONS = 960.0)
 DENS (SET = "tissue", CONS = 200.0)
 SPEC (SET = 1, CURV = 22, TEMP)
```

-0.2600000000E+03, -0.5000000000E+02, -0.2890000000E+02, -0.2330000000E+02,
-0.1780000000E+02, -0.1220000000E+02, -0.9400000000E+01, -0.6700000000E+01,
-0.5600000000E+01, -0.4400000000E+01, -0.3900000000E+01, -0.3300000000E+01,
-0.2800000000E+01, -0.2200000000E+01, -0.1700000000E+01, -0.1100000000E+01,
0.1700000000E+01, 0.4400000000E+01, 0.7200000000E+01, 0.1000000000E+02,
0.1560000000E+02, 0.4500000000E+02, 0.2321000000E+04, 0.2321000000E+04,
0.2321000000E+04, 0.2332142857E+04, 0.2709090909E+04, 0.3607142857E+04,
0.5321428571E+04, 0.8703703704E+04, 0.1327272727E+05, 0.1758333333E+05,
0.2940000000E+05, 0.3216666667E+05, 0.5260000000E+05, 0.6550000000E+05,
0.8340000000E+05, 0.3000000000E+04, 0.3000000000E+04, 0.3518518519E+04,
0.3178571429E+04, 0.3214285714E+04, 0.3160714286E+04, 0.3160000000E+01
COND (SET = "Tumor", CONS = 1.401)
COND (SET = "Lung", CONS = 0.245)
BCNO (TEMP, ENTI = "PROTUM", CONS = -190.0)
BCFL (HEAT, ENTI = "TUMB", CONS = 0.000000000000E+00)
BCFL (HEAT, ENTI = "LUNGB", CONS = 0.000000000000E+00)
BCFL (HEAT, ENTI = "TUML", CONS = 0.000000000000E+00)
BCFL (HEAT, ENTI = "LUNGL", CONS = 0.000000000000E+00)
BCFL (HEAT, ENTI = "LUNGEND", CONS = 0.000000000000E+00)
ICNO (TEMP, CONS = 37.0, ENTI = "TUMORFACE")
ICNO (TEMP, CONS = 37.0, ENTI = "LUNGFACE")
END
/ *** of FIPREP Commands
CREATE(FIPREP,DELE)
CREATE(FISOLV)
PARAMETER(LIST)

Convergence of Mesh

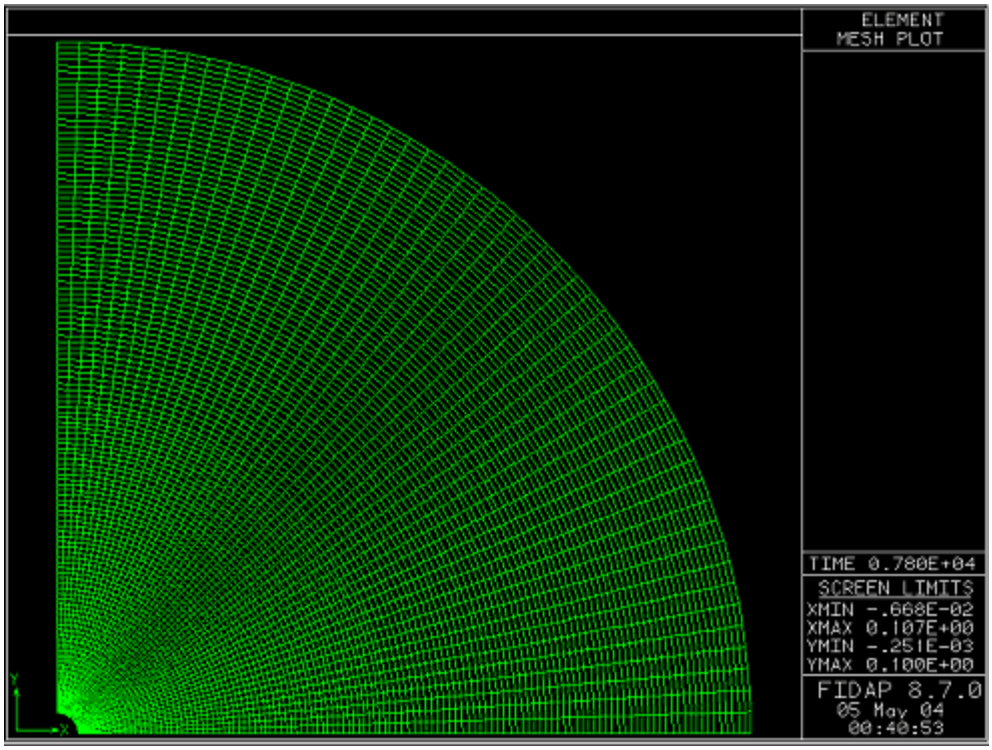

Figure 16. The refined mesh used in the convergence analysis.

Contours of temperature at various times

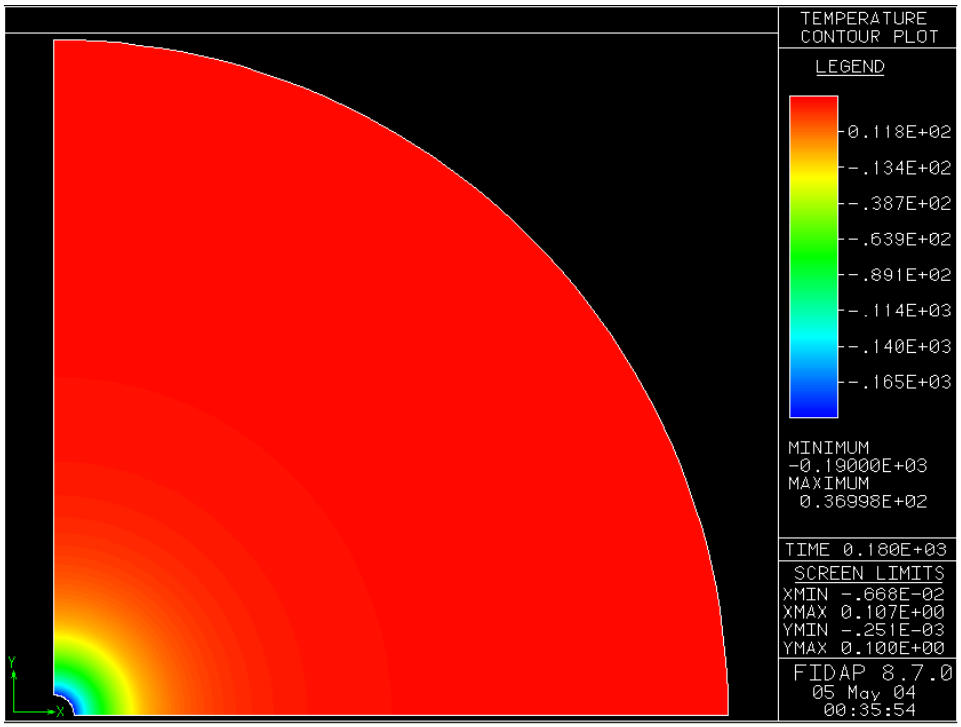

Figure 17. Temperature contour at time = 180 seconds.

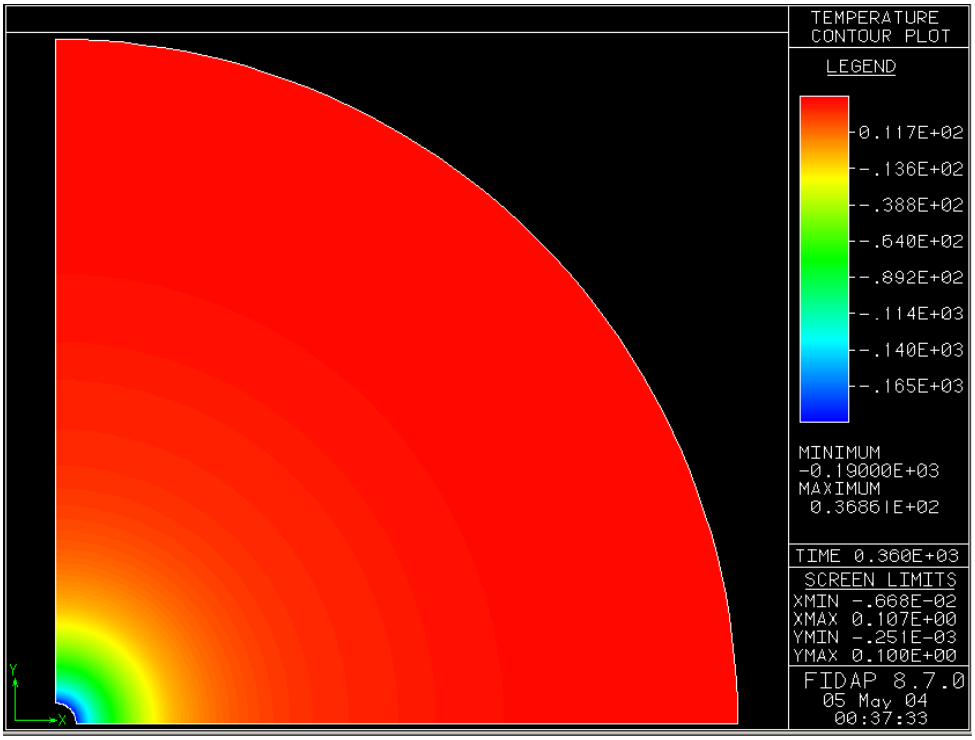

Figure 18. Temperature contour at time = 360 seconds.

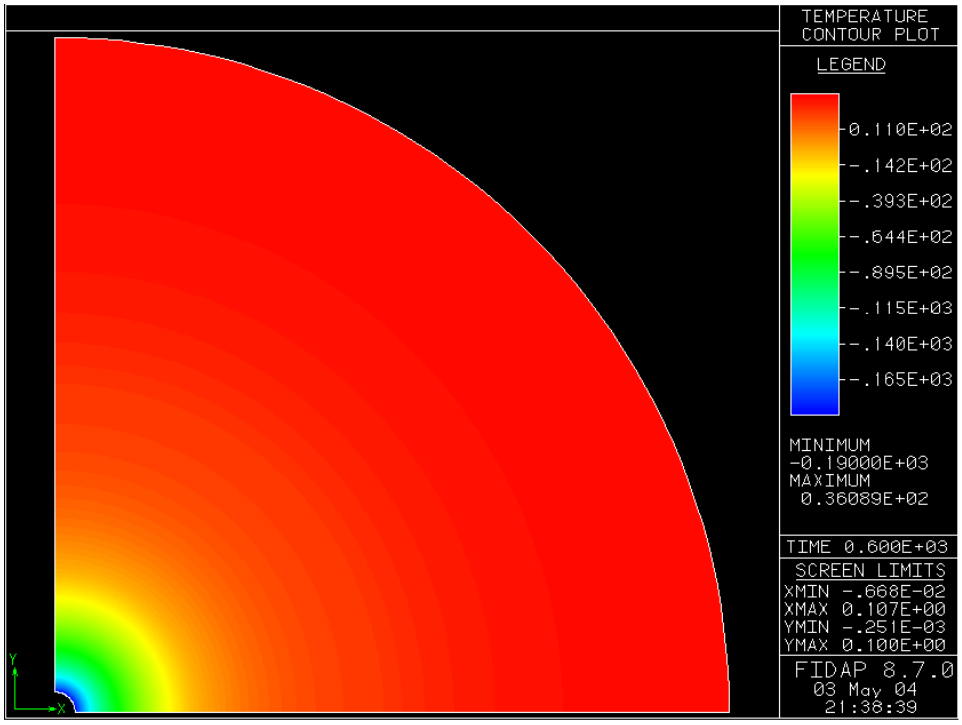

Figure 19. Temperature contour at time = 600 seconds.

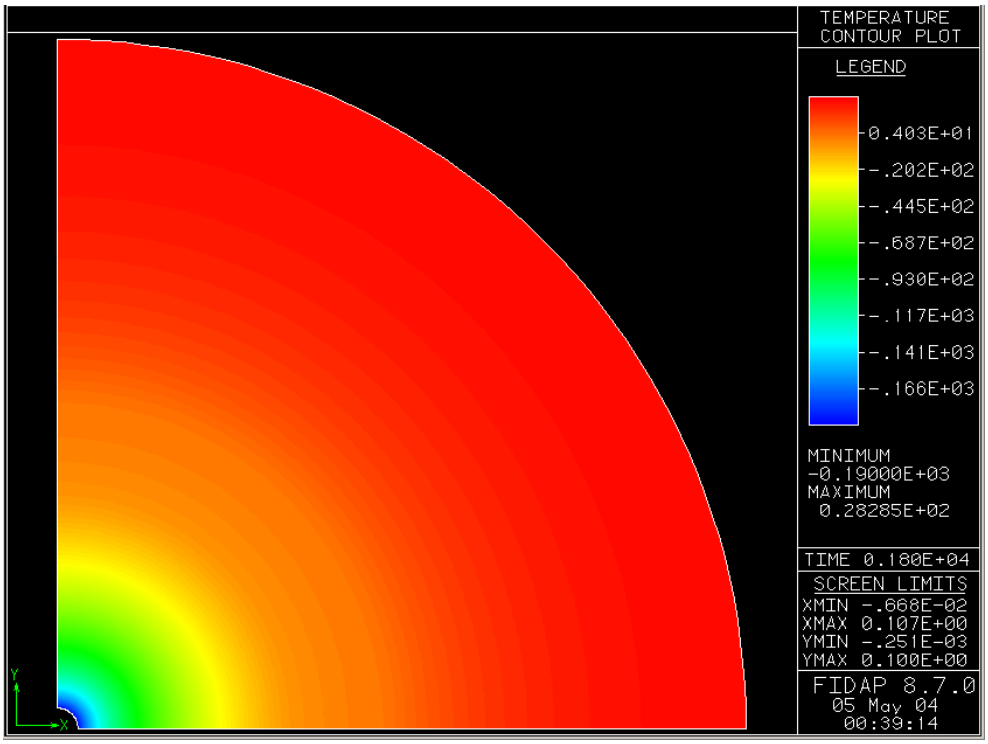

Figure 20. Temperature contour at time = 1800 seconds.

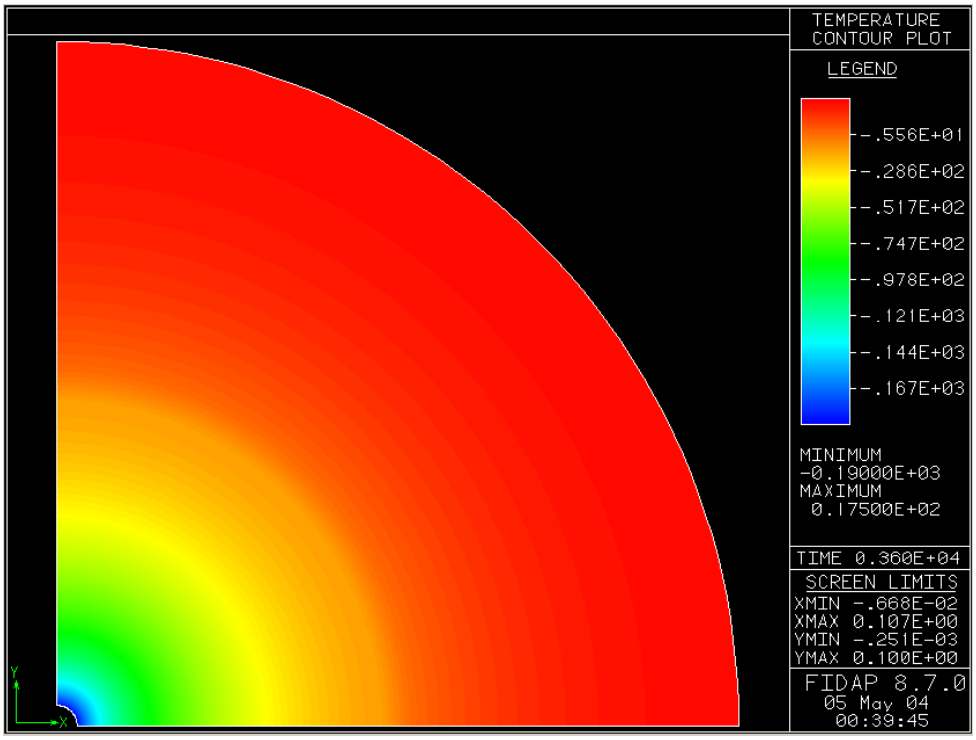

Figure 21. Temperature contour at time = 3600 seconds.

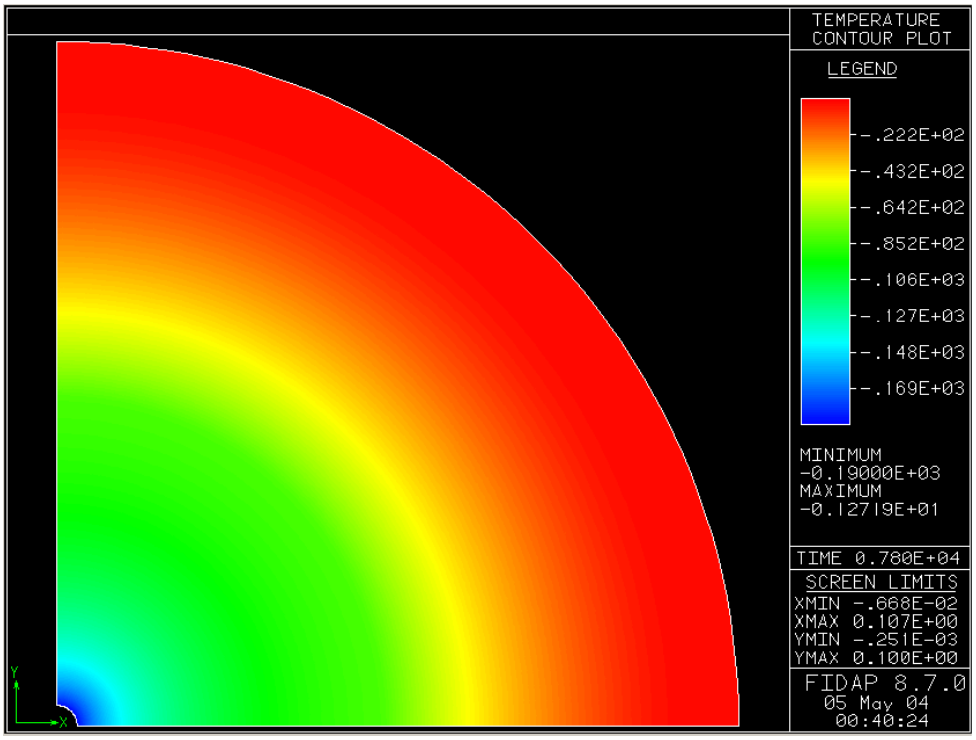

Figure 22. Temperature contour at time = 7800 seconds.

Temperature History Plots

A comparison of these graphs with the original graphs confirms that there is no significant difference and that the mesh has converged.

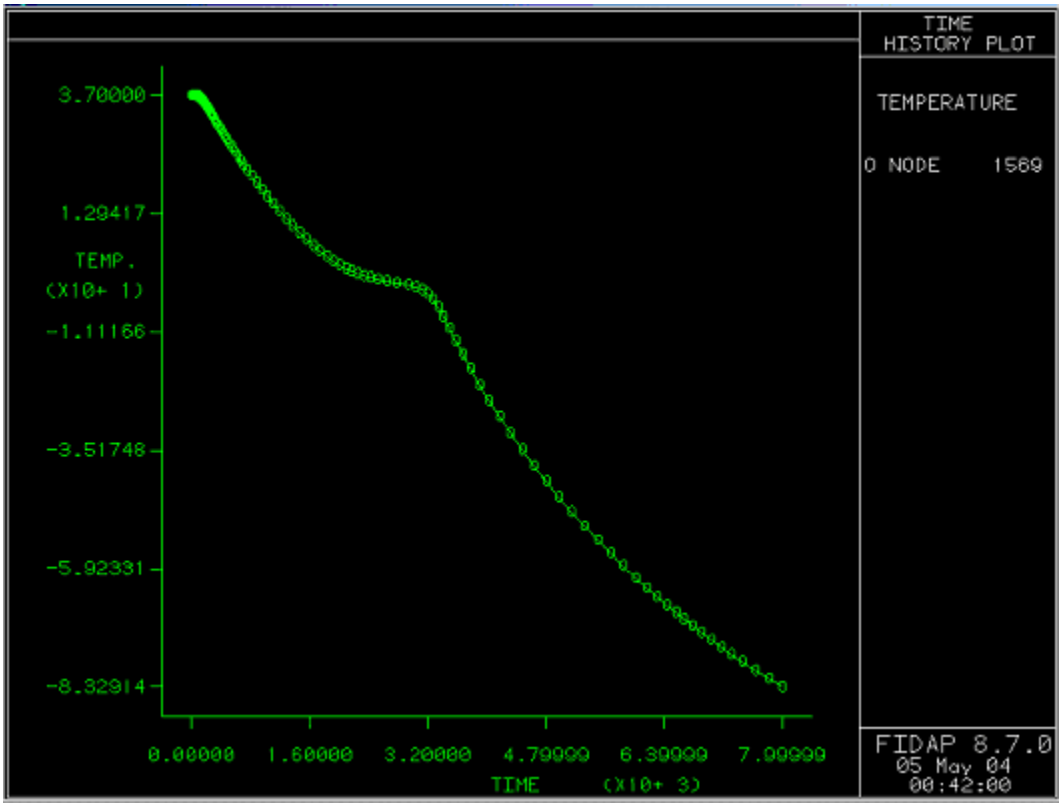

Figure 23. Temperature history plot at node 1569 on the outer edge of the tumor.

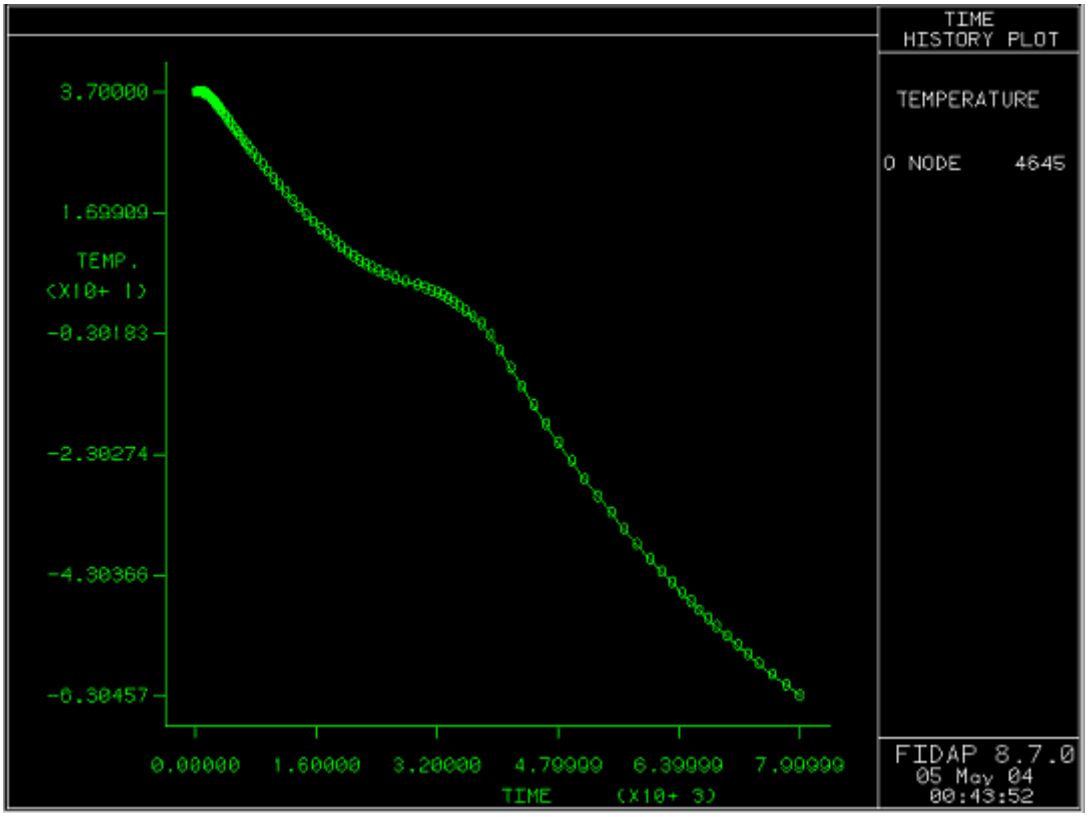

Figure 24. Temperature history plot at node 4645 on the inner edge of the healthy tissue.

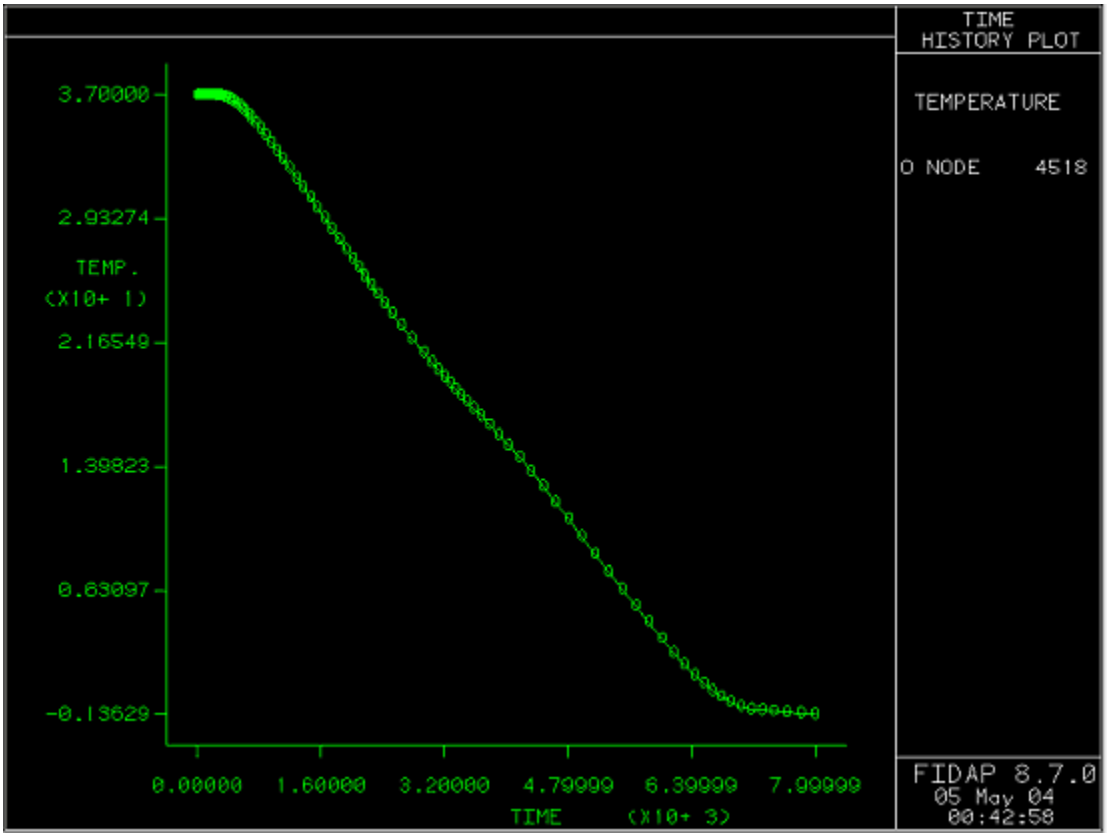

Figure 25. Temperature history plot at node 4518 on the outer edge of the healthy tissue.

Appendix C

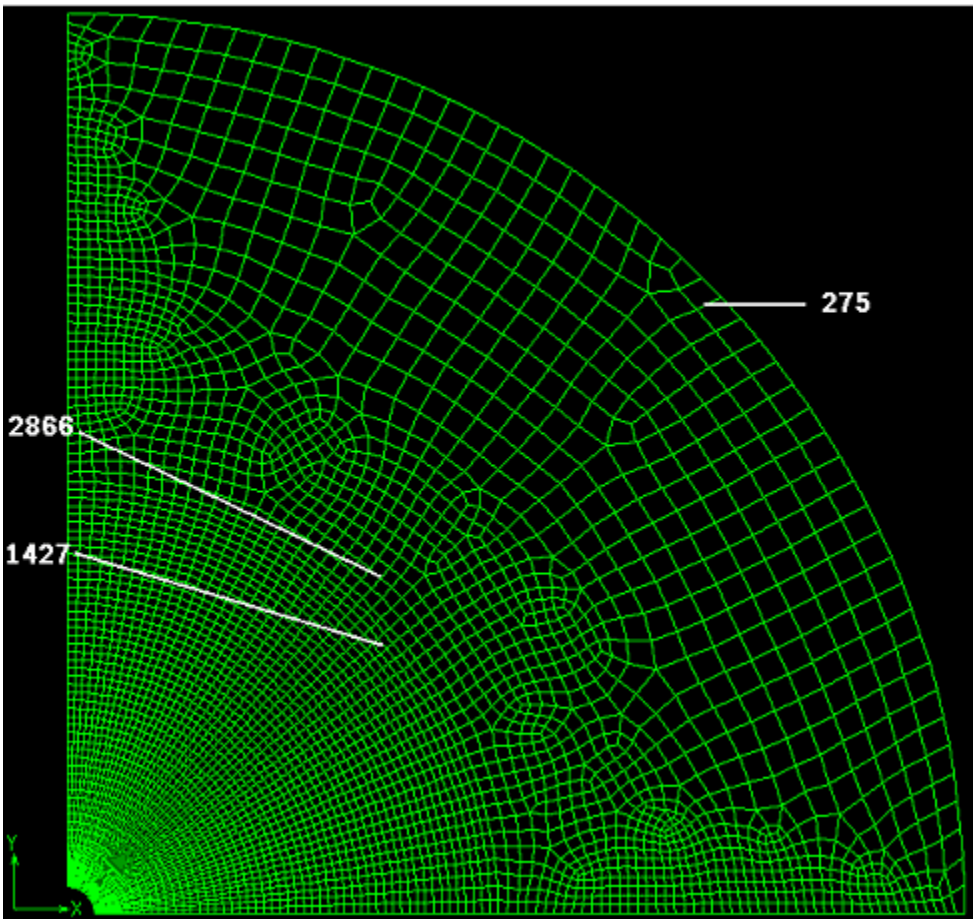

Figure 26. Location of the nodes used in the temperature history plots.

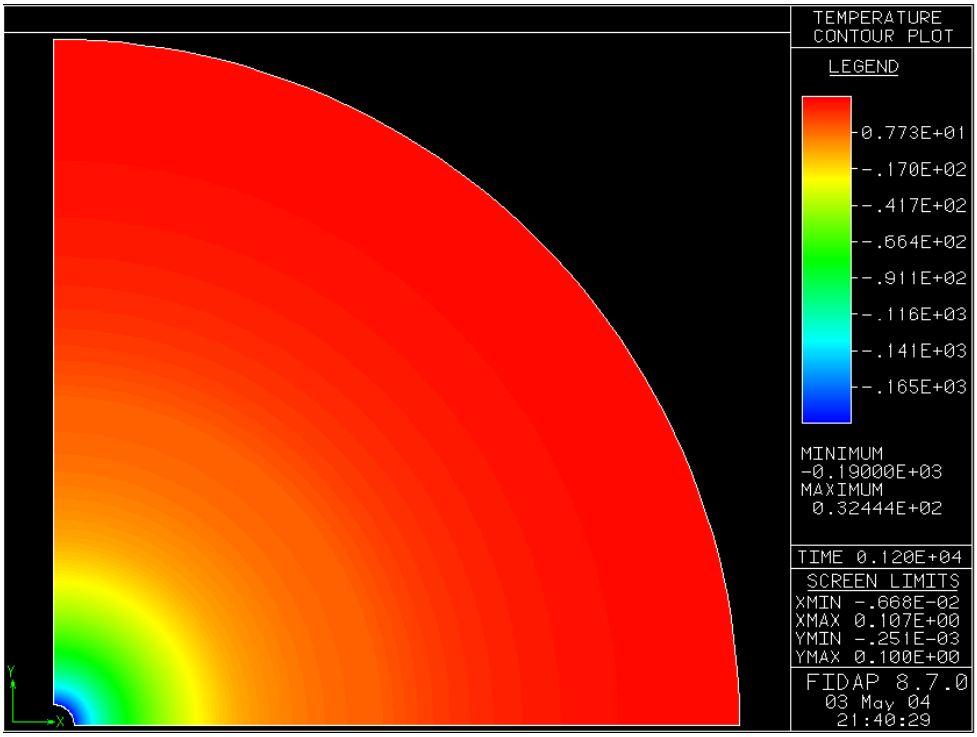

Figure 27. Temperature contour plot used in analyzing the original model; probe application time = 20 minutes.

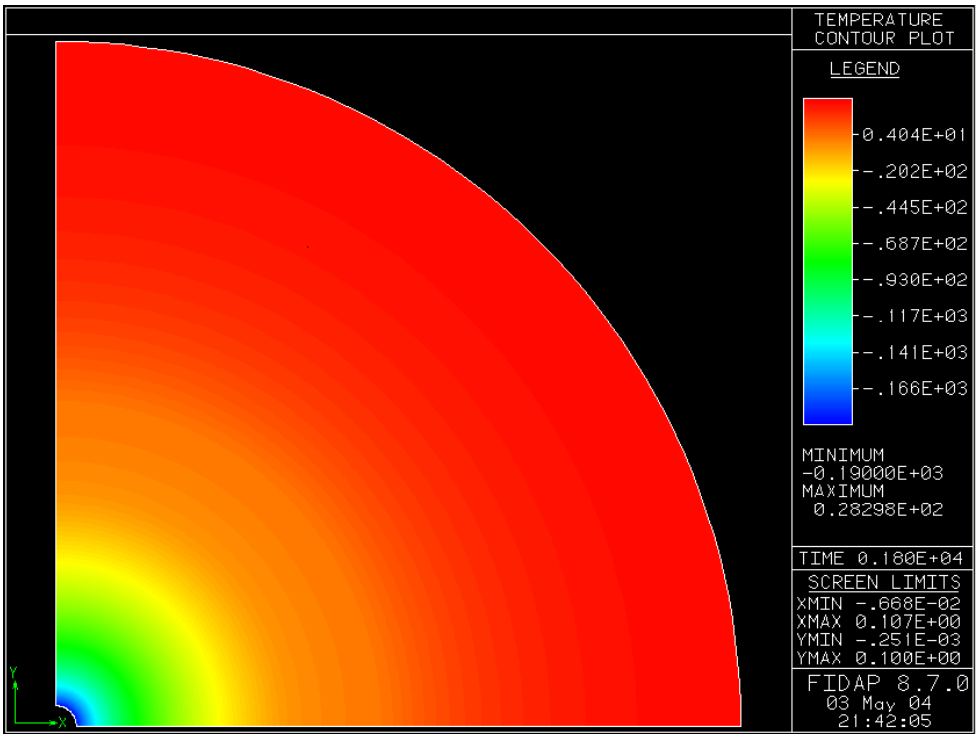

Figure 28. Temperature contour plot used in analyzing the original model; probe application time = 300 minutes.

.

The following graphs display the original temperature history profile used in calculating the optimal application time.

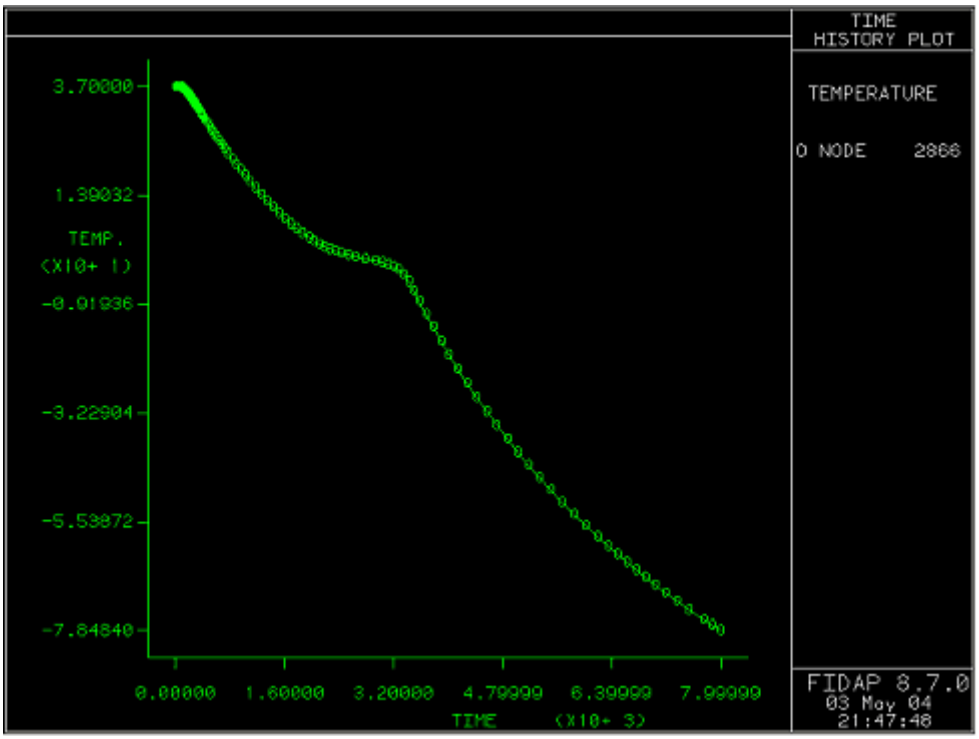

Figure 29. Temperature history plot for node 2866 on the inner edge of the healthy tissue.

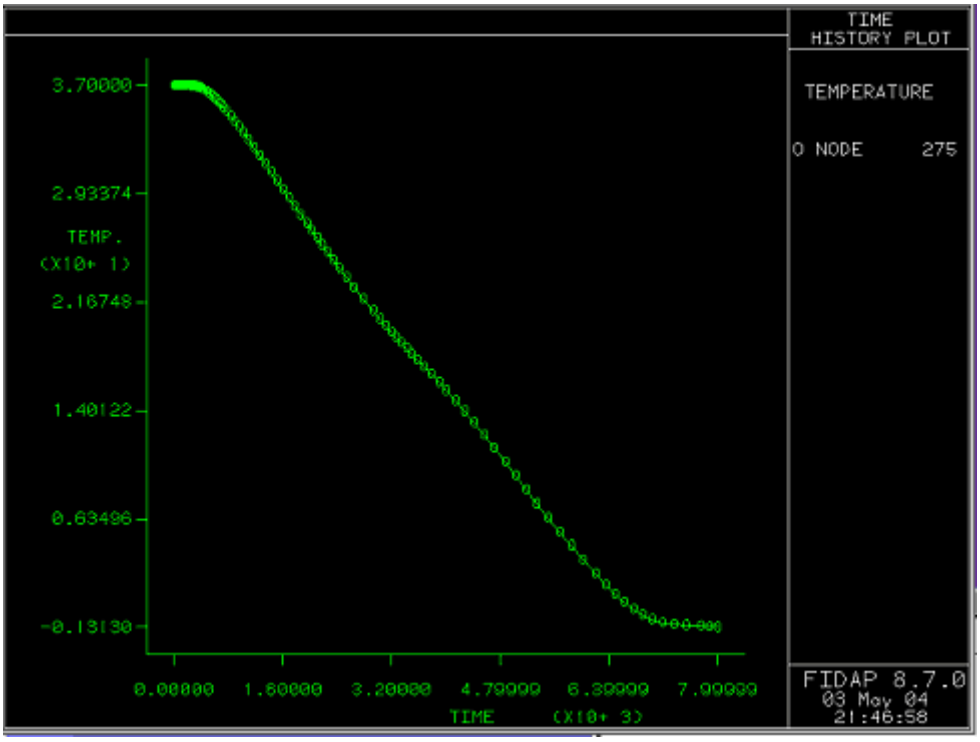

Figure 30. Temperature history plot for node 275 on the outer edge of the healthy tissue.

When determining the sensitivity of the model to probe temperature the following contours were consulted.

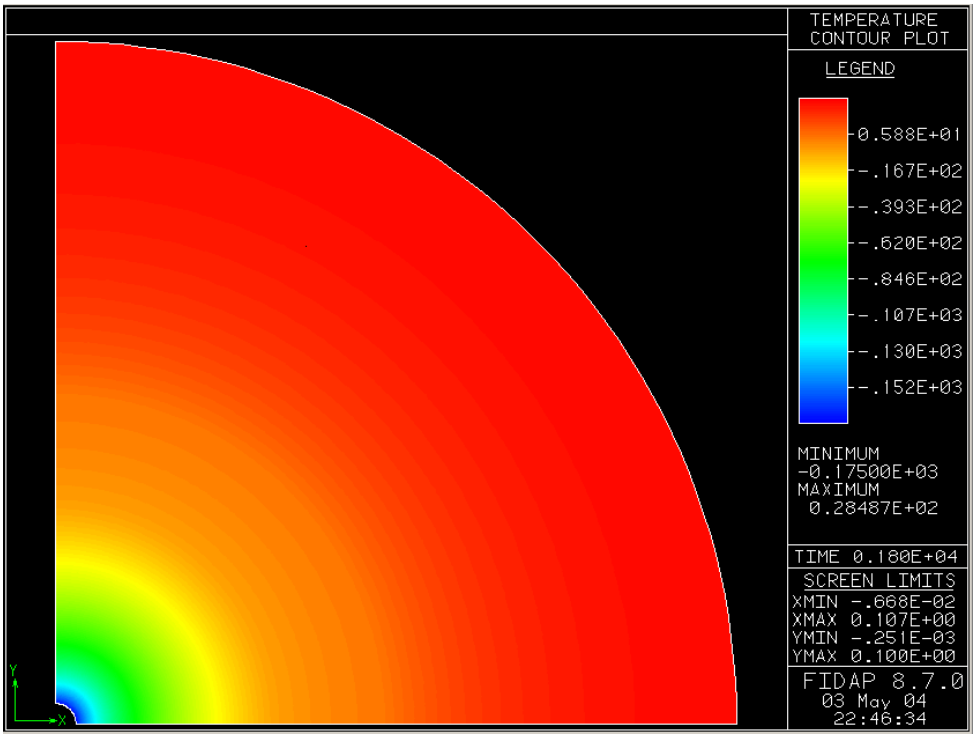

Figure 31. Temperature contour plot after application of a –175°C probe for 30 minutes.

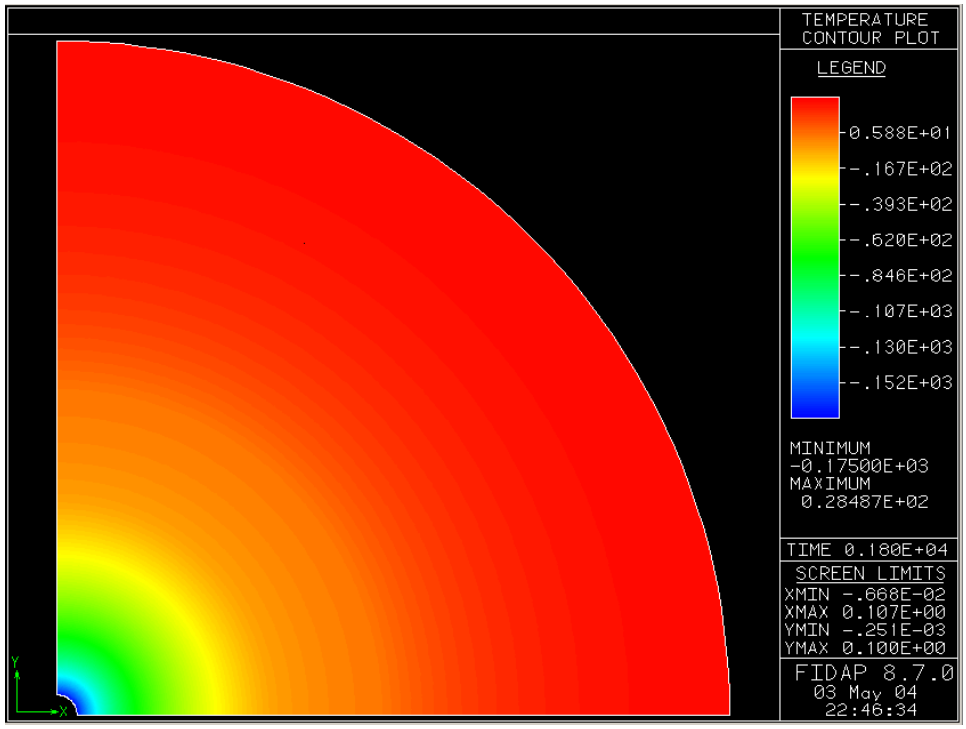

Figure 32. Temperature contour plot after application of a –240°C probe for 30 minutes.

When determining the sensitivity of probe temperature the following temperature history plots were also consulted.

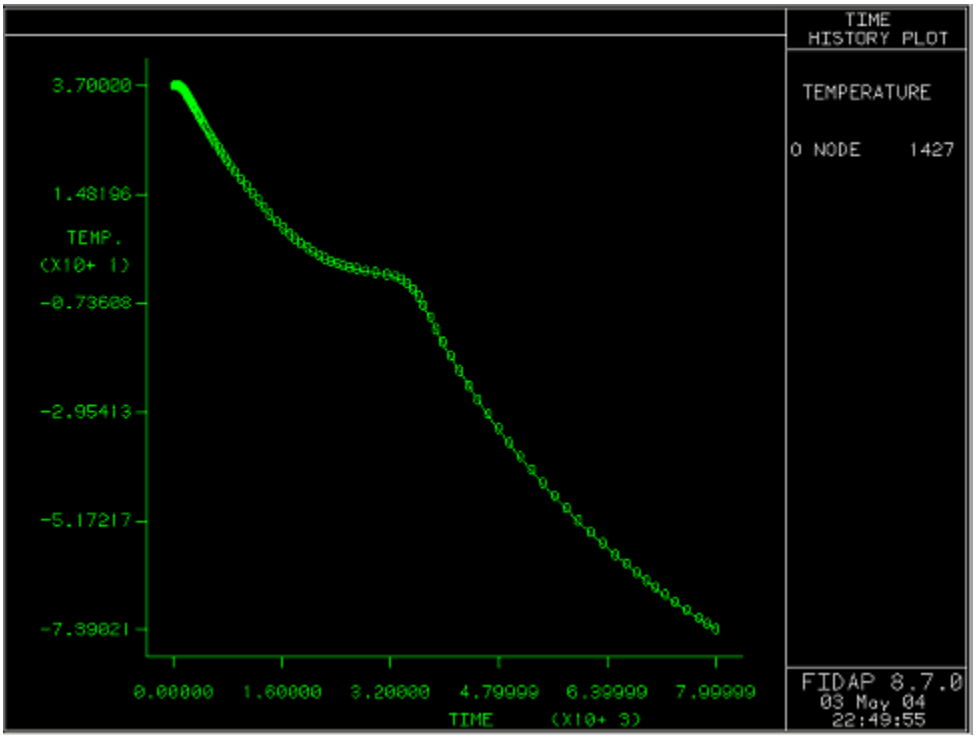

Figure 33. Temperature history of node 1427 at the outer edge of the tumor tissue with a probe of –175 °C.

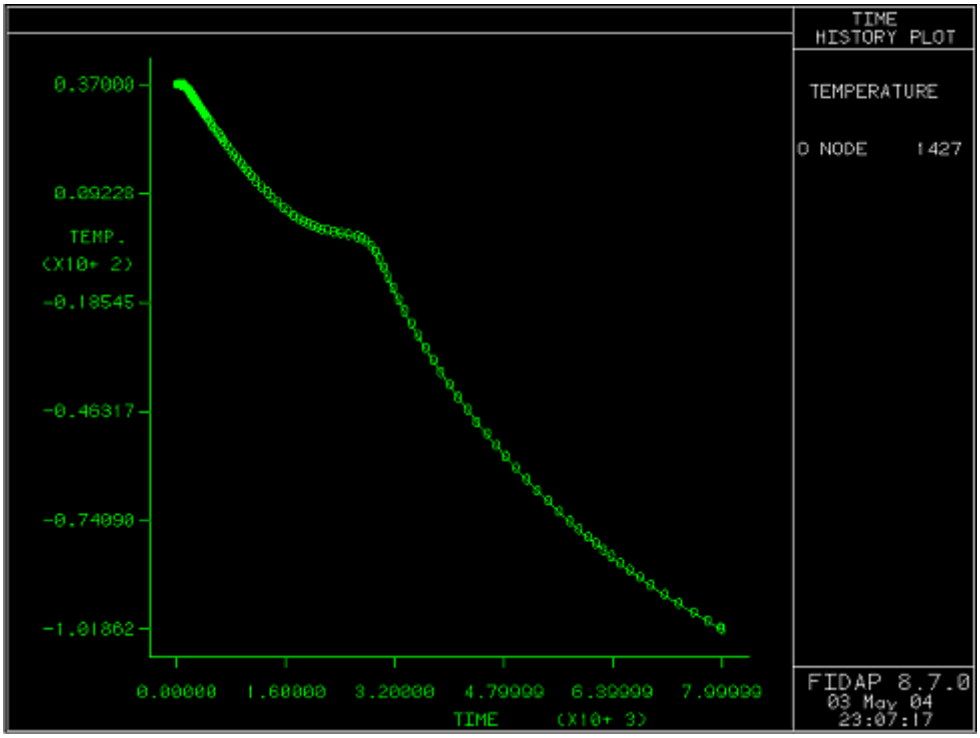

Figure 34. Temperature history of node 1427 at the outer edge of the tumor tissue with a probe of –220 °C.

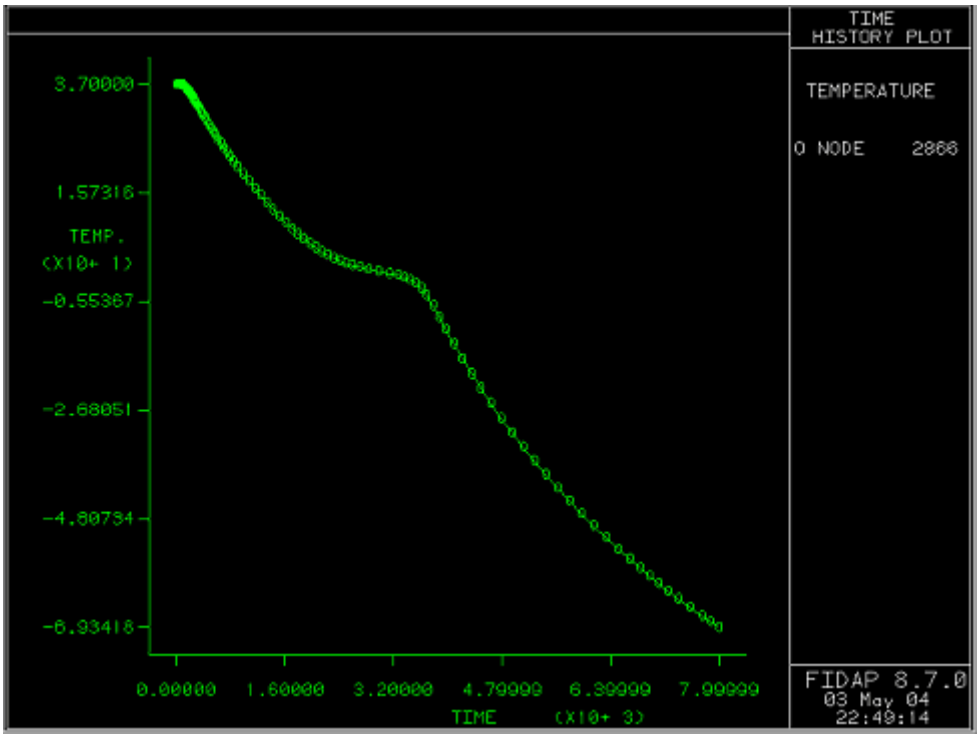

Figure 35. Temperature history of node 2866 on the inner edge of the healthy tissue with a probe temperature of –175°C.

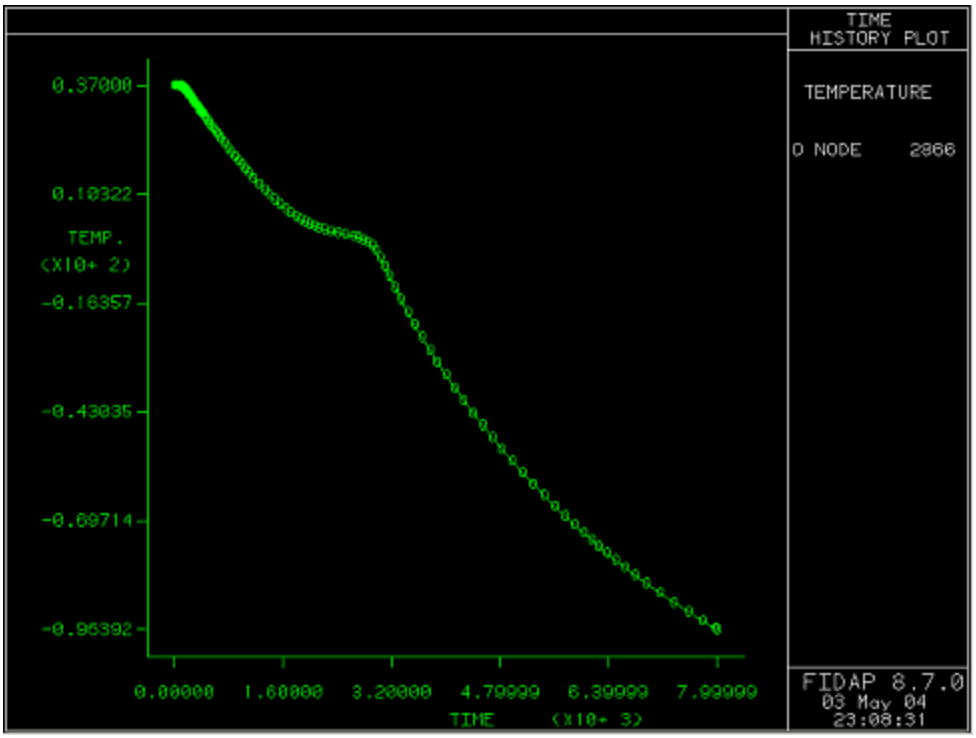

Figure 36. Temperature history of node 2866 at the outer edge of the tumor tissue with a probe temperature of –220°C.

Next we also consulted temperature history plots after changes in density.

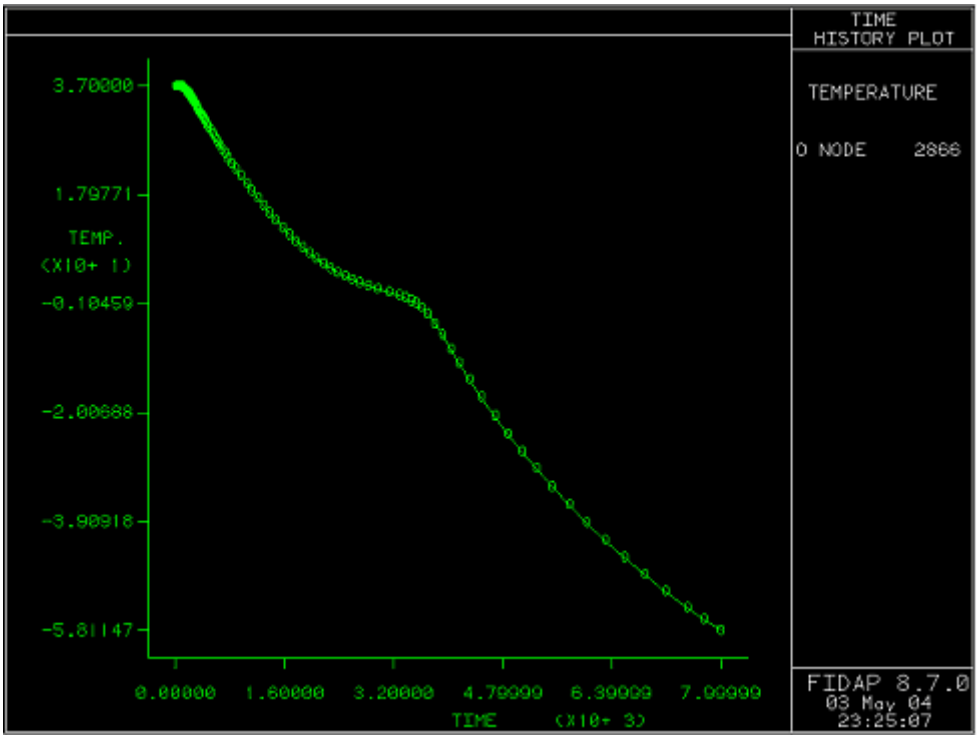

Figure 37. Temperature history of node 2866 at the outer edge of the tumor tissue, when the healthy tissue has a density = 500 kg/m^3.

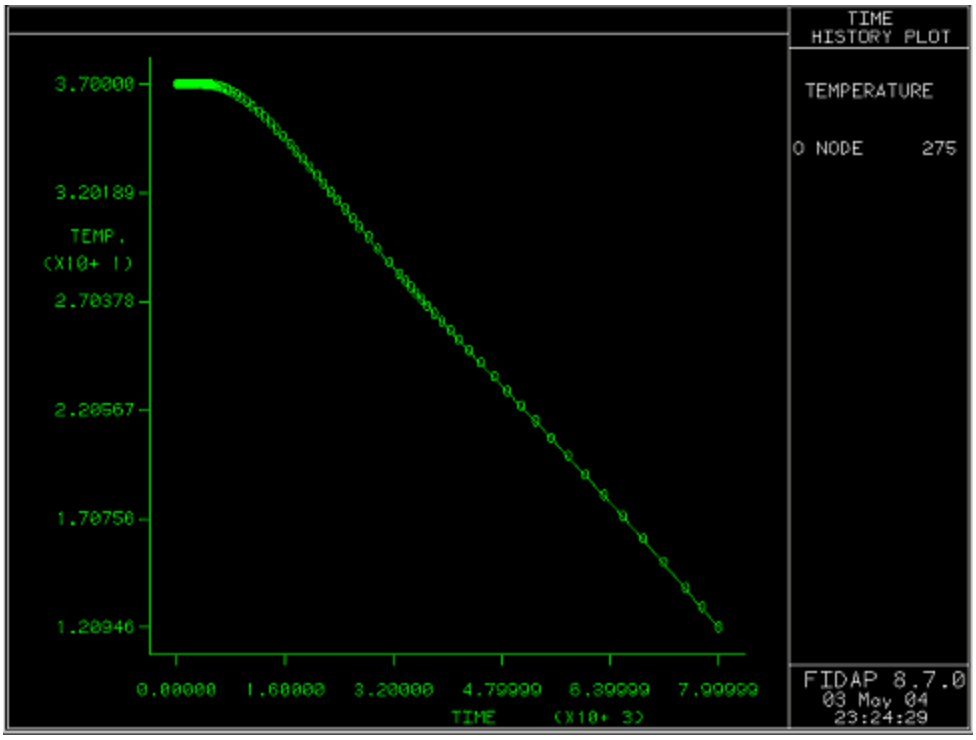

Figure 38. Temperature history of node 275 at the outer edge of the healthy tissue, when it has a density = 500 kg/m^3.

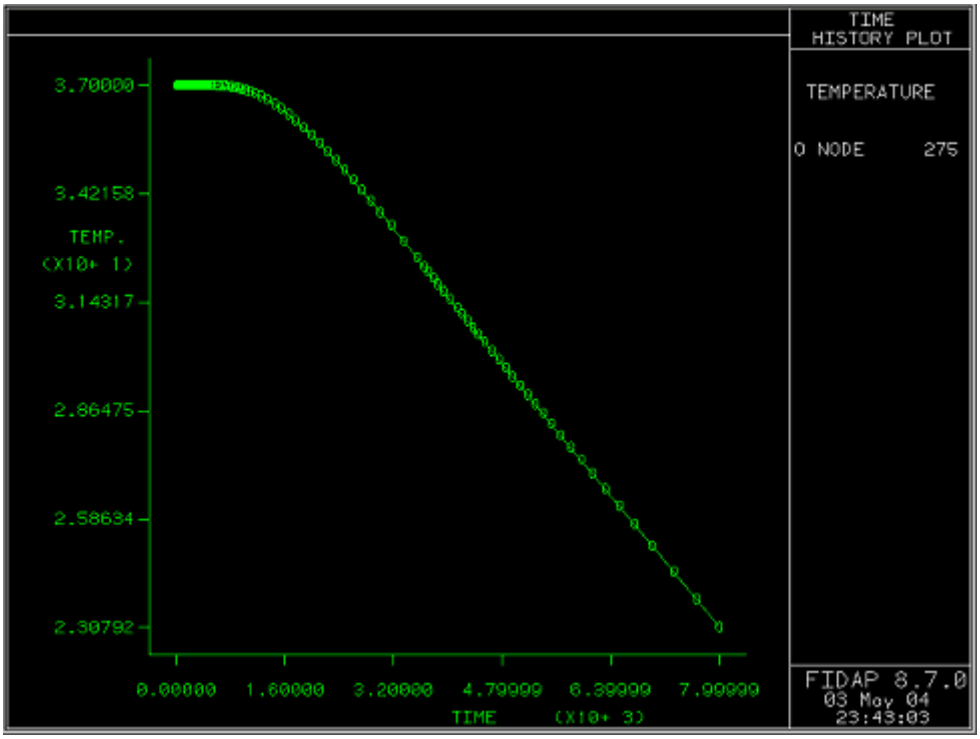

Figure 39. Temperature history of node 275 at the outer edge of the healthy tissue, when it has a density = 1000 kg/m^3.

Appendix D: References

[i] National Cancer Institute. "Cancer.gov.: Lung Cancer Home Page" 2 May 2004. http://www.cancer.gov/cancer_information/cancer_type/lung/

[ii] J.P. Homasson, P. Renault, M. Angebault, J.P. Bonniot, and N.J. Bell, *Chest,* **2**, 159 (1990)

[iii] W.S. Wong, D.O. Chitin, and TL Wynnmian, *Cancer.* **79**. 963 (1997)

[iv] J.P. Homasson. *Eur Repir .J*, **2**, 799 (1989)

[v] G.T. Anderson, J.W. Valvano. L.J. Hayes. and C.H. White. *Computational Methods in Bioengineering,* R. L. Spilker and B. R. Simon. Eds., AS.ME.. New York. 301 (1988).

[vi] Datta, A.K. 2003. *Computer-Aided Engineering: Applications to Biomedical Processes*. Department of Biological and Environmental Engineering, Cornell University, Ithaca, New York.

[vii] eGeneralMedical.com. "Brymill Cryogenic Systems: Cryosurgery Equipment" 6 May 2004 http://egeneralmedical.com/brymcryogsys.html

[viii] Anthony Products, Inc. "Cryosurgery Equipment" 6 May 2004 http://www.anthonyproducts.com/equipment/dermasurgical/cryosurgery/cryosurgery.htm

[ix] R. J. Schweikert and R. G. Keanini. *Int. Comm. Heat Mass Transfer*. **26**, 1 (1999)

[x] E. Malvica, B. Salter, K. Verma, T. Watkins, M. Shauhgnesy. *Cryopreservation of the Kidney: A Feasible Study Based on Cooling Rates*. Department of Biological and Environmental Engineering, Cornell University, Ithaca, New York. (2003)